MECHANISMS AND THERAPEUTIC APPLICATIONS OF
TIME-VARYING AND STATIC MAGNETIC FIELDS

Arthur A. Pilla

Department of Biomedical Engineering, Columbia University, New York, NY 10032

Department of Orthopedics, Mount Sinai School of Medicine, New York, NY 10029

INTRODUCTION

It is now commonplace to learn of the successful use of weak non-thermal electromagnetic fields (EMF) in the quest to heal, or relieve the symptoms of, a variety of debilitating ailments. This review will attempt to give the reader an introduction and assessment of EMF modalities which have demonstrated therapeutic benefit for bone and wound repair and chronic and acute pain relief. This review will concentrate on the use of exogenous time-varying and static magnetic fields. There is, however, a large body of research, including many clinical studies, describing the successful application of electrical signals via electrodes in electrochemical contact with the skin for pain relief and to enhance wound repair. Consideration of these modalities is beyond the scope of this review. The reader is referred to several excellent reviews of such electrical stimulation modalities (1-5). Electroporation (6-8,372), which applies high amplitude (>100V/cm), short duration (≤1 msec), voltage pulses with electrodes in contact with the target, allows controlled transient opening of the cell and other membranes, and has shown promise for gene transvection (9) and treatment of certain cancers (10), is also beyond the scope of this review. Finally RF (>100 MHz) and microwave signals are also beyond the scope of this review since these modalities are rarely utilized to enhance bone or wound repair, but rather for tissue heating, thermal ablation or as surgical tools. Non-thermal bioeffects at these frequencies have been reported, but there are many controversial findings. Excellent reviews are available for the reader interested in more detail (11,373).

1

As of this writing there are a considerable number of peer-reviewed publications which show EMF can result in physiologically beneficial *in vivo* and *in vitro* bioeffects. The number of people who have received substantial clinical benefit from exogenous EMF is certainly in the millions worldwide and increasing rapidly as new clinical indications emerge. EMF therapies also present as alternatives to many pharmacologic treatments with virtually no toxicity or side effects. Time-varying electromagnetic fields consisting of rectangular or arbitrary waveforms, referred to as pulsing electromagnetic fields (PEMF), pulse modulated radio frequency waveforms, particularly in the 15–40 MHz range, referred to as pulsed radio frequency fields (PRF) and low frequency sinusoidal waveforms (< 100 Hz) have been shown to enhance healing when used as adjunctive therapy for a variety of musculoskeletal injuries. Indeed, peer-reviewed meta-analyses clearly show both PEMF and PRF modalities, now approved by regulatory bodies worldwide and widely used on patients to enhance bone and wound repair, are clinically effective (12-13). Although still not completely elucidated, the mechanism of action of EMF signals at the molecular and cellular level is now much better understood and strongly suggests ion/ligand binding in a regulatory cascade could be the signal transduction pathway (14-28). Furthermore, *a priori* configuration of physiologically effective waveforms via tuning the electrical properties of the exogenous EMF signal to the endogenous electrical properties of ion binding has recently been reported (29-30).

This chapter will provide a brief overview of the basic and clinical evidence that time-varying magnetic fields (EMF) can modulate molecular, cellular and tissue function in a physiologically significant manner. The fundamental questions relating to the biophysical conditions under which EMF signals could modulate cell and tissue function will be discussed in detail. Particular attention will be paid to the manner by which signal parameters are related to dosimetry. In other words, the properties which render an EMF signal bioeffective. An attempt is made to correlate dosimetry for weak magnetic field with that for electric field effects. The ratio of signal to (endogenous) thermal noise (SNR) in the target is used in a SNR/Dynamical Systems model which has been successful for the *a priori* configuration of physiologically significant waveforms and which the reader may find useful to decipher the myriad of waveforms that have been utilized. The model may also allow

the reader to perform an *a posteriori* analysis of waveforms for dose related explanations for the presence or absence of a biological effect. Examples of *in vivo* and *in vitro* studies are given, illustrating specific EMF waveforms, including several examples of the use of the model.

TISSUE REPAIR

1.0 Orthopedic Applications

Five million bone fractures occur annually in the United States alone. About 5% of these will become delayed or nonunion fractures with associated loss of productivity and independence (31). Several techniques are available to treat recalcitrant fractures such as internal and external fixation, bone grafts or graft substitutes including demineralized bone matrix, platelet extracts and bone matrix protein, and biophysical stimulation, such as mechanical strain applied through external fixators or ultrasound, and electromagnetic fields.

The electrical properties of bone tissue have been extensively investigated. Yasuda in Japan hypothesized that endogenous electrical activity observed in bone was the mediator of repair and adaptive remodeling responses to mechanical loading and that an exogenous electrical signal alone could stimulate the response (32,33). A seminal report soon followed on bone piezoelectric properties from the pioneering work of Fukada and Yasuda (34). These authors showed a voltage could be obtained upon deformation of dry bone. Several groups, notably led by Becker at the State University of New York, Bassett at Columbia University and Brighton at the University of Pennsylvania, soon reported the generation of electrical potentials in wet bone on mechanical deformation (35-39). Similar observations were subsequently made in collagen and cartilaginous tissues (40-43). The important conclusion from these studies was the revelation that bone and other tissue could respond to electrical signals in a physiologically useful manner. This ultimately led to the use of electromagnetic fields to modulate bone repair.

The development of modern EMF therapeutics was stimulated by the clinical problems associated with non-union and delayed union bone fractures. It started with the pioneering work of Yasuda, Fukada, Becker, Brighton, and Bassett, mentioned above, who responded to the

fundamental orthopedic question of how bone adaptively and structurally responds to mechanical input by suggesting that an electrical signal may be involved in the transduction of the mechanical signal to cellular activity. This naturally led to the suggestion that superimposing an exogenous EMF upon the endogenous fields accompanying normal cellular activity could help in the treatment of difficult fractures. The first animal studies employed microampere level DC currents delivered via implanted electrodes. Remarkably, this resulted in new bone formation particularly around the cathode (44). As these studies progressed it became clear that the new bone growth resulted from the chemical changes around the electrodes caused by electrolysis (45). However, it has been shown that a mechanical stimulus also plays a role in DC bone stimulation (46). The first therapeutic devices were based on these early animal studies and used implanted and semi-invasive electrodes delivering DC to the fracture site (47,48). This was followed by the development of clinically preferable externally applied electromagnetic field modalities (49-52). Subsequent studies concentrated on the direct effects of electromagnetic fields leading to modalities which provided a non-invasive, no-touch means of applying an electrical/mechanical signal to a cell/tissue target. Therapeutic uses of these technologies in orthopaedics have led to clinical applications, approved by regulatory bodies worldwide, for treatment of recalcitrant fractures and spine fusion (53-59) and recently for osteoarthritis of the knee (60-62). Additional clinical indications for EMF have been reported in double blind studies for the treatment of avascular necrosis (63,64) and tendinitis (65). This spectrum of applications clearly demonstrates the potential of this biophysical modality to enhance musculoskeletal tissue healing.

At present, the clinical modalities in use for bone repair consist of electrodes implanted directly into the repair site or noninvasive capacitive or inductive coupling. Direct current (DC) is applied via one electrode (cathode) placed in the tissue target at the site of bone repair and the anode placed in soft tissue. DC currents of 5-100 μA are sufficient to stimulate osteogenesis (45). The capacitive coupling (CC) technique utilizes external skin electrodes placed on opposite sides of the fracture site (66). This requires openings in the cast or brace to allow skin access. Sinusoidal waves of 20 to 200 kHz are typically employed to induce 1-100 mV/cm electric fields in the repair site (67). The inductive coupling (PEMF) technique induces a time-varying electric field at the repair

site by applying a time-varying magnetic field via one or two electrical coils. The induced electric field parameters are determined by frequency characteristics of the applied magnetic field and the electrical properties of the tissue target (15,30,50,51). Several waveform configurations have been shown to be physiologically effective. Peak time-varying magnetic fields of 0.1 - 20 G, inducing 1-150 mV/cm peak electric fields in a 3 cm diameter target, have been used (50,68). The relationship between inductively coupled waveform characteristics and their ability to produce physiologically significant bioeffects will be considered in detail below. One version of the inductive technique utilizes a specific combination of DC and AC magnetic fields (CMF) that are believed to tune specifically to ion transport processes (17).

1.1 Cellular Studies

Cellular studies have addressed effects of electromagnetic fields on both signal transduction pathways and growth factor synthesis. The important overall result from these studies is that EMF can stimulate the secretion of growth factors (e.g., insulin-like growth factor-II) after a short duration trigger stimulus. The clinical benefit to bone repair is enhanced production of growth factors upregulated as a result of the fracture trauma. The induced electric field thus acts as a triggering mechanism which modulates the normal process of molecular regulation of bone repair mediated by growth factors.

Studies underlying this working model have shown effects on calcium ion transport (69), a 28% increase in cell proliferation (70), a fivefold increase in IGF-II release (71), and increased IGF-II receptor expression in osteoblasts (72). Increases of 53% and 93% on IGF-I and II respectively have also been demonstrated in rat fracture callus (73). Stimulation of TGF-β mRNA by threefold with PEMF in a bone induction model in the rat has been reported (74). This study also suggests the increase in growth factor production by PEMF may be related to the induction of cartilage differentiation (75). It also suggests the responsive cell population is most likely mesenchymal cells (76), which are recruited early in the duration of PEMF stimulus to enhance cartilage formation. Upregulation of TGF-β mRNA by 100%, as well as collagen, and osteocalcin synthesis by PEMF has been reported in the human osteoblast-like cell line MG-63 (77,78). PEMF

stimulated a 130% increase in TGF-β1 in bone non-union cells (79). That the upregulation of growth factor production may be a common denominator in the tissue level mechanisms underlying electromagnetic stimulation is supported by studies from the Brighton (80,81) Stevens (82) and Aaron (83) groups.

Using specific inhibitors, the Brighton group suggests EMF acts through a calmodulin-dependent pathway (81). This follows reports by the Pilla group (84-90) that specific PEMF and PRF signals, as well as weak static magnetic fields, modulate Ca^{2+} binding to CaM by a twofold acceleration in Ca^{+2} binding kinetics in a cell-free enzyme preparation. The Stevens group has shown upregulation of mRNA for BMP2 and BMP4 with PEMF in osteoblast cultures. The Aaron group has reported extensively on upregulation of TGF-β in bone and cartilage with PEMF. All of these studies have utilized EMF signals identical to those which have demonstrated clinical success. The ion binding target pathway has recently been confirmed in other studies using static magnetic fields (91,92). PEMF has been reported to increase angiogenesis by threefold in an endothelial cell culture (93). A recent study confirms this and suggests PEMF increases *in vitro* and *in vivo* angiogenesis through a sevenfold increase in endothelial release of FGF-2 (94).

1.2 Animal Studies

Bassett et al. (95,96) were the first to report a PEMF signal could accelerate bone repair by 150% in a canine tibial osteotomy model. A bilateral cortical hole defect model in the metacarpal bones in horses showed PEMF treated holes produced a statistically significant increase in amount of new bone formation and mineral apposition rate (97,98). A capacitively coupled signal was shown to prevent osteopenia due to both sciatic-denervation and castration in rat osteopenia models (99,100). PEMF inhibited bone loss in an ovariectomized canine model (101). Combined magnetic fields reversed osteopenia in ovariectomized rats (102). An avian ulna disuse model showed a significant increase in bone formation when treated with PEMF (103). The frequency dependence of EMF effects was also studied in this model. The results showed maximal response was observed with a 15 Hz sinusoidal waveform producing 10 μV/cm peak electric field in tissue. Experimental models of bone repair show enhanced cell proliferation, calcification, and increased mechanical

6

strength with DC currents (104,105). Capacitive coupled fields have been reported to improve the mechanical strength of experimental fractures and healing osteotomies (67). Several studies with PEMF showed increased calcification and enhanced mechanical strength in healing bone (106,107). Exposure time studies report a linear effect of daily exposure with a 6-hour stimulation being most effective (68). A series of animal studies reported that DC, CC, and PEMF techniques enhance the formation of bone and improves fusion rates in spinal arthrodeses (108-110). DC currents of 10 μA per cm of cathode length showed the best acceleration of spinal fusion (111). The mechanical strength of late phase osteotomy gap healing in the dog was 35% stronger in PEMF treated limbs (112). PEMF increased bone ingrowth into hydroxyapatite implants in cancellous bone by 50% (113). PEMF produced a 10% increase in the diameter of arteriolar microvessels in rat muscle from which the authors suggested increased local blood flow could play a role in the PEMF acceleration of bone repair (114). The use of in vivo micro-computed tomography showed PEMF reduced bone loss in a non-union fibular model in the rat by threefold (363). In a related study the effect of PEMF waveform configuration was examined. The results showed callus stiffness in a rat fibular osteotomy was increased twofold by a PEMF signal routinely employed for clinical bone repair, whereas a second PEMF waveform with much higher frequency content was ineffective (369).

1.3 Clinical Studies

Electromagnetic stimulation modalities have been used clinically to treat fresh fractures, osteotomies, spine fusions, and delayed and nonunion fractures. The efficacy of EMF stimulation on bone repair has been studied in a formal meta-analysis (12). Twenty randomized control trials were identified. Fifteen trials supported EMF effectiveness and five failed to show effectiveness. Most studies used PEMF. In all cases, the primary outcome measure was bone healing assessed by radiographs and clinical stability test. Results from pooled trials of 765 cases supported the effectiveness of PEMF stimulation of bone repair. However, because of the inability to pool data from all studies, conclusions regarding PEMF efficacy in bone repair were only suggestive. PEMF significantly accelerated union of femoral and tibial osteotomies in randomized, placebo controlled studies by approximately 50% (115-117).

PEMF, CC and DC have been used to promote healing of spine fusions for the treatment of chronic back pain from worn or damaged intervertebral discs. This is measured by the increase in successful fusions from 50% to approximately 80% using EMF as adjunctive treatment. This application has also been subjected to meta-analysis (13). Five randomized, controlled trials and five nonrandomized case controlled studies showed positive results for the enhancement (by 60%) of spine fusion by electrical and electromagnetic stimulation. There are many studies and reviews which show electrical and electromagnetic stimulation is effective in promoting spinal arthrodesis (118-122).

The effectiveness of EMF in promoting healing of recalcitrant fractures has been reviewed (123). Twenty-eight studies of ununited tibial fractures treated with PMF were compared with 14 studies of similar fractures treated with bone graft with or without internal fixation. The overall success rate for the surgical treatment of 569 ununited tibial fractures was 82%, while that for PMF treatment of 1718 ununited tibial fractures was 81%, suggesting it is significantly more advantageous for the patient to use PEMF rather than submit to invasive surgery for the first bone graft. There are several observational studies suggesting the efficacy of DC, CC, or PEMF techniques in stimulating healing of delayed unions and nonunions (124-132). Interestingly, Bone morphogenetic proteins. Development and clinical efficacy in the treatment of fractures and bone defects. and of huge clinical significance, studies comparing PEMF with bone graft show their equivalence in promoting union of delayed union or nonunion fractures (123,133-135). Finally, there is a promising study on the effects of PEMF on distraction osteogenesis for the correction of bone length discrepancies (136).

Thus, several physical modalities have been shown to effectively manage nonunions and delayed unions of bone. Implantable direct current stimulation is effective as an adjunct in achieving spinal fusion. Pulsed electromagnetic fields induce weak non-thermal time-varying currents at the fracture site. Inductively and capacitively coupled electromagnetic fields appear to be as effective as surgery in managing extremity nonunions and lumbar and cervical fusions. Low-intensity ultrasound has also been used to speed normal fracture healing and manage delayed unions.

Although these modalities seem vastly different, there appears to be a common mechanism of action. This will be discussed below.

All of the modalities discussed above now constitute the standard armamentarium of orthopaedic clinical practice. Since the success rate for these modalities has been reported equivalent to that for the first bone graft, a huge advantage to the patient ensues because PEMF therapy is non-invasive and is performed on an out-patient basis. PEMF therapy also provides significant reductions in the cost of health care since no operative procedures or hospital stays are involved. This also applies for the increased success rate of spinal fusions with EMF. Thus, the clinical effects of EMF on hard tissue repair are physiologically significant and often constitute the method of choice when standard of care has failed to produce adequate clinical results. It is interesting to note that EMF may be the best modulator of the release of the growth factors specific to each stage of bone repair, certainly more so than the exogenous application of the same growth factors (398).

2. Soft Tissue Applications

Chronic wounds and their treatment are an enormous burden on the healthcare system, both in terms of their cost ($5 billion to $9 billion annually) and the intensity of care required (137). There is even more cost to society from attendant human suffering and reduced productivity. More than 2 million people suffer from pressure ulcers and as many as 600,000 to 2.5 million more have chronic leg and foot wounds (137). Diabetic foot ulcers are the most common chronic wounds in western industrialized countries. Of the millions who have diabetes mellitus, 15 per cent will suffer foot ulceration which often leads to amputation (100,000 per annum in the US alone).

There is an emerging and substantial clinical application of EMF in wound healing. Soft tissue healing has been reported by the use of direct electrode coupled devices delivering waveforms similar to those produced by several TENS devices currently approved by the FDA (5). Regulatory and reimbursement issues have prevented more widespread use of PEMF modalities. However, the clear clinical effectiveness of PEMF signals has resulted in significantly increased use (12). In fact,

the Center for Medicare Services (CMS) has now determined PEMF produces sufficient clinical outcome to permit, and reimburse for, use in the off-label application of healing chronic wounds, such as pressure sores and diabetic leg and foot ulcers (138). In addition, PRF devices have been cleared by the FDA for the relief of acute and chronic pain and the reduction of edema, all symptoms of wounds from post surgical procedures, musculoskeletal injuries, muscle and joint overuse, as well as chronic wounds.

As for bone repair, application of EMF to soft tissue repair appears to have begun with observations of the electrical events associated with wound repair (139-143). Injury currents which develop in the presence of dermal wounds are postulated to play an important role in the healing process (144-145). These currents are, however, at least two orders of magnitude larger than the endogenous currents from SGP and are DC, or near DC, currents. Cells involved in wound repair are electrically charged and endogenous DC currents may facilitate cellular migration to the wound area (146-147). In a manner similar to that for bone repair, the original working hypothesis was that exogenous EMF signals may enhance the endogenous electrical signals to accelerate wound repair. It has also been suggested that externally applied EMF may interact with the current of injury or trigger a relevant growth factor cascade (148,149). Wound healing can be accelerated 2.5 fold with 200-800 µA direct current (150). Both DC current and PEMF have been reported to reduce edema, increase blood flow, modulate upregulated growth factor receptors, enhance neutrophil and macrophage attraction and epidermal cell migration, and increase fibroblast and granulation tissue proliferation (147,149). Most wound studies involve arterial or venous skin ulcers, diabetic ulcers, pressure ulcers and surgical and burn wounds.

2.1 Cellular and Animal Studies

The PEMF signal currently utilized for bone repair (see figure 2, top) accelerates vascularization by several fold using cells from human umbilical vein and bovine aorta (151). Studies on human umbilical vein cells showed that endothelial cell migration to a wounded area is accelerated by about 14% if cell cultures are exposed to an induced electrical field similar to the pulse burst currently used for bone repair (2 mT peak, 25 Hz repetition rate) (151). Chronic stimulation of rat

muscles increased blood vessel density by 14-30%, possibly through angiotensin and vascular endothelial growth factor pathways (152). PEMF produced a significant increase in the rate of growth of the vascular tissue in the rabbit ear chamber (153) showing a dependence on signal configuration (repetitive pulse burst significantly better than repetitive single pulse). Sinusoidal signals (300 Hz) improved microcirculation and stimulated proliferation and differentiation of fibroblasts (154). Amplitude, frequency and orientation dependence of EMF modulation of fibroblast protein synthesis has been reported (155). Inductively coupled sinusoidal fields (0.06-0.7 mT, 50, 60 and 100 Hz) increased chick embryo fibroblast proliferation up to 64% (156). Human fibroblasts exposed to 20 or 500 mT 50 Hz sinusoidal signals exhibited no effect on fibroblast proliferation (157). Fibroblasts exposed to a PRF signal consisting of a 65 μsec burst of 27.12 MHz sinusoidal waves repeating at 600/sec (1G peak amplitude) showed enhanced cell proliferation by 130-220% (158,159). Tissue cultures of human foreskin fibroblasts, when exposed to high 2 V/cm induced electric fields at either 1 or 10 Hz, demonstrated a six-fold increase in internal calcium, but excitation at 100 Hz had no significant effect (160). Recent animal studies have reported that PRF signals produced a statistically significant several fold increase in neovascularization in an arterial loop model, suggesting an important clinical application for angiogenesis (161,162). PRF signals, configured *a priori* assuming a Ca/CaM transduction pathway, accelerated wound repair in a rat cutaneous wound model by approximately 60% as measured by tensile strength (163). However, treatment of identical wounds in the rat with PEMF of the type and intensity used for bone healing (see Figure 2, top) failed to produce significant increases in soft tissue fibroblast counts or improvement in wound closure (164). PEMF increased the degree of endothelial cell tubulization and proliferation (threefold) in vitro (94). In the same study PEMF increased fibroblast growth factor β-2 by fivefold from which the authors conclude that PEMF augments angiogenesis primarily by stimulating endothelial release of FGF-2.

2.2 Clinical Studies

Non-thermal PRF signals were originally utilized for the treatment of infections in the pre-antibiotic era (165) and are now widely employed for the reduction of post-traumatic and post-operative pain and edema. Double-blind clinical studies have been reported for chronic wound

repair, wherein PRF treated pressure ulcers closed by 84% vs 40% closure in untreated wounds in one study (166) and 60% closure vs no closure in the control group in another study (167); acute ankle sprains, wherein edema decrease was sevenfold vs the control group (168,169); and acute whiplash injuries, wherein pain decreased by 50% and range of motion increased by 75% in the treated vs control patients (170,171). PRF signals have been reported to enhance skin microvascular blood flow by about 30% in both healthy (172) and diabetic (173) individuals. PRF reduced postmastectomy lymphedema by 56% and increased skin blood flow fourfold (174). PEMF at 600 and 800 Hz, 25 µT mean amplitude, significantly reduced the size of venous ulcers by 63%, and decreased pain by 72%, in a randomized control study (175). A modulated EMF signal at 10 and 100 Hz relieved the main clinical symptoms of diabetic peripheral neuropathy, improved peripheral nerve conduction by about 40% and the reflex excitability of functionally diverse motoneurons in the spinal cord (176).

A meta-analysis was performed on randomized clinical trials using PEMF on soft tissues and joints (12). The results showed both PEMF and PRF were effective in accelerating healing of skin wounds (177-183), soft tissue injury (168-171,184) and hair regrowth (185-187), as well as providing symptomatic relief in patients with osteoarthritis and other joint conditions (61,62). PEMF has been successfully used in the treatment of chronic pain associated with connective tissue (cartilage, tendon, ligaments and bone) injury and joint-associated soft tissue injury (188,189).

As for bone repair, EMF clinical effects on soft tissue repair are substantial and often constitute the method of choice when standard of care has failed to produce adequate clinical results. This is particularly true for chronic wounds which often do not respond to standard of care and can be life-threatening if not resolved. It is interesting to note that EMF can increase angiogenesis several fold in chronic wounds, significantly more than that achieved to date with growth factors such as VEGF (vascular endothelial growth factor), for which there have been generally disappointing clinical results (399). This may be the primary reason that EMF is so effective with problem wounds wherein increased blood supply is always one of the primary clinical objectives. It is also

interesting to note that EMF can provide an alternative to NSAIDs (e.g., ibuprofen, cox2 inhibitors, etc.) and other pharmacological analgesics for the relief of chronic and acute pain.

BIOPHYSICAL CONSIDERATIONS OF EMF THERAPEUTICS

3.0 Introduction

The above sections have provided an overview of the abundance of *in vitro*, *in vivo* and clinical evidence which suggest time-varying magnetic fields of various configurations can produce physiologically beneficial effects for conditions as varied as chronic and acute pain, chronic wounds and recalcitrant bone fractures. This has all been achieved with low intensity, non-thermal, non-invasive time-varying electromagnetic fields, having many configurations over a very broad frequency range. The reader should be aware that pulsing ultrasound (US) and intermittent mechanical loading have also been shown to modulate bone repair and remodeling (190-198). It has been suggested (199-201) that an ion binding transduction pathway is common to both mechanical and EMF modalities which provides useful US signal dosimetry information. This will be further discussed below. There is also compelling evidence that weak static magnetic fields can provide physiologically useful musculoskeletal pain relief (202-209). Here also, ion binding may be involved in the transduction pathway via the effect of weak magnetic fields on the motion dynamics of the bound ion (19-26,210-216). This can modulate binding kinetics by accelerating bound ions to preferred active orientations within the binding site or channel. Static magnetic fields as low as 10 µT can be detected in this pathway if the ion remains bound on the order of a second. One model, based upon Larmor precession of the bound ion, predicts static magnetic field effects as well as windows for certain combinations of AC and DC magnetic fields, similar to the ion cyclotron and parametric resonance models, as will be shown below (211-213).

Clearly, many EMF signals appear to have the capacity to achieve a physiologically meaningful bioeffect. Why should such seemingly different doses be effective? Are any signal parameters better than others? Is it the magnetic or electric field, or both? Does the state of the tissue target

13

play a role? Despite the understandable impression that many EMF signals have been chosen in some arbitrary manner, the following sections will attempt to show that EMF dosimetry can have a rigorous quantitative basis based upon relatively simple mechanisms.

The biophysical mechanism(s) of interaction of weak electric and magnetic fields on biological tissues as well as the biological transductive mechanism(s) have been vigorously studied. One of the first models was created using a linear physicochemical approach (14,15,29,30,49,50,223, 224,233) in which an electrochemical model of the cell membrane was employed to predict a range of EMF waveform parameters for which bioeffects might be expected. This approach was based on the assumption that voltage dependent processes, such as ion/ligand binding and ion transport at and across the electrified interface of the cell membrane were the most likely EMF targets. Several elegant studies further quantified this approach using Lorentz force considerations (16-19), including ion resonance and the Zeeman-Stark effect (20). These suggested combined low frequency AC and DC magnetic fields could modulate ion/ligand movement in a molecular cleft (binding site) and thereby affect binding kinetics (19-26,210-216). Direct action of the Lorentz force on free electrons in macromolecules such as DNA has also been proposed (217-219).

At present, the most generally accepted biophysical transduction step is ion/ligand binding at cell surfaces and junctions which modulate a cascade of biochemical processes resulting in the observed physiological effect (81,83,220,225). A unifying biophysical mechanism which could explain the vast range of reported results and allow predictions of which EMF signals and exposures are likely to induce a clinically meaningful physiological effect has been proposed (29,30).

Electromagnetic bioeffects from relatively weak (below heating and excitation thresholds) signals can be produced with a time-varying electric field, E(t), induced from an applied time-varying magnetic field, B(t). A large number of electromagnetic clinical devices in present use (particularly for bone and wound repair) induce 1-100 mV/cm peak E at the treatment site (12,13,68). A myriad of waveforms have been employed and the fundamental question becomes one of dosimetry. In

other words, the relation of waveform configuration to detectability (dose) at the supposed target must be established. The first step is evaluation of the amplitude and spatial dosimetry of the induced EMF within the target site for each exposure system and condition. This has been rigorously carried out for the laboratory dish with coils oriented vertically or horizontally (226-228). Models have been created for the distribution of induced voltage and current in human limbs (229) and joints (230). Three dimensional visualizations of clinical PEMF signals have been reported (362).

3.1 Inductively Coupled Clinical EMF Waveforms

The electric field induced via a time-varying magnetic field waveform is directly related to the electrical characteristics of the coil employed and the current waveform applied to the coil. Induced electromotive force (emf) is proportional to the rate of change of current in the coil (dI_{coil}/dt) which produces the shape of the induced electric field. The following is applicable to coils which have been utilized for clinical bone fracture repair.

Coil current $I_{coil}(t)$ for an air-core inductor driven with a voltage step V_O rises exponentially to the limiting current defined by the coil resistance, as:

$$I_{coil}(t) = (V_O / R_{coil})[1 - \exp(-t\,R_{coil} / L)] \tag{1}$$

where L is the coil inductance and R_{coil} is the effective coil resistance, including all connecting cable and driving circuit resistances. The waveform of the induced voltage is a direct function of the time derivative of $I_{coil}(t)$:

$$dI_{coil} / dt = V_O / L \, \exp(-t\,R_{coil} / L) \tag{2}$$

Equation 2 clearly shows that a rectangular-type induced waveform is achieved for a linear rise in coil current if τ_{coil} (= L/R_{coil}) is sufficiently greater (e.g., by 10 times) than the rise time of current in the coil. This can be achieved by the proper choice of L and R_{coil}. One modality is to keep L relatively small so that safe driving voltages (<25 V) can be employed. Note that, as given by Eq. 2, the maximum induced voltage (as $t \rightarrow 0$) is inversely proportional to coil inductance for a given V_O. Effective coil resistance can be kept small by utilizing heavy magnet wire and connecting

15

cable (e.g., 14-16 B&S gauge). With the above taken into account it is easy to see that, for a given R_{coil}, the voltage step (V_O) can be applied to the coil for as long as the following relation is approximately valid:

$$(dI_{coil} / dt)_{t \to 0} = V_O / L [1 - (t R_{coil} / L)]$$

(3)

Equation 3 shows coil current will rise approximately linearly resulting in an induced voltage waveform in the form of a "step" having some negative slope, as shown in figure 1.
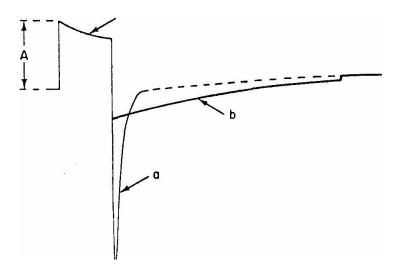

Figure 1: Schematic illustration of an inductively coupled electric field waveform used for bone and wound repair. The coil time constant (L/R_{coil}) determines the shape of this signal during rise of current in the coil. Collapse of coil current can be diode-limited (b) or determined by the impedance of the electronic driving circuitry (a). [From Pilla et al., J Biol Phys. 1983;11:51-57, with permission.]

At the time of coil turn-off coil current must collapse back to zero. This can be accomplished in either of two manners. In the first, the coil current is allowed to decay at a rate determined only by the coil and driving circuit impedance (a, figure 1). In the second, rate of current collapse is controlled by an amplitude-limiting diode (b, figure 1). By using either of these modes, induced waveform patterns having similar or different opposite polarity durations and amplitudes can be achieved.

16

The waveform shown in figure 1 represents the electric field induced in the cell/tissue target via a coil placed external to the skin surface. Some of the pulse-type induced electric field waveforms in common clinical use are shown in figure 2. The rationale behind the configuration of these waveforms was based on the assumption that the induced electric field (and associated induced current density) is the primary stimulus. In other words, the magnetic component was considered to be the carrier or coupler, not significantly contributing to the biological effect. That this is correct for many PEMF clinical signals will become evident below. Clinical EMF signals for bone repair are inductively coupled, except for one capacitive coupled 60 kHz sinusoidal signal, for which E dosimetry, estimated from the geometry and dielectric properties of the target (121), is in the mV/cm peak range. There is also the continued and anomalous use of invasive DC currents, despite the accompanying electrolytic effects which are known to cause bone formation via an inflammatory response (39-41).
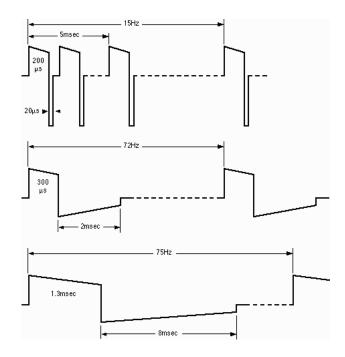

Figure 2: Induced electric field, E(t), in tissue from the time-varying magnetic fields utilized in EMF devices for clinical applications. The top waveform consists of bursts of asymmetrical pulses; the others are wide asymmetrical single pulses. For all signals peak E is 1-10 mV/cm in a 2 cm target. All are detectable by some tissue targets. Positive clinical effects have been reported for all signals.

The waveforms shown in figures 1 and 2 represent the time variation of the electric field signal induced in the extracellular fluid/cell/tissue complex in a human, animal or plant target. The distribution of current flow depends upon the geometry of coil and target. The basic rule is that the voltage induced will be defined by the distribution of magnetic flux within the tissue and the electrical properties of the target. To illustrate, consider a pair of Helmholtz aiding circular coils. A plastic culture dish, having cylindrical geometry, can be placed between the coils such that the symmetry (z) axis is aligned with that of the coils (see figure 3). The $z = 0$ plane passes through the mid-plane of a saline solution, of conductivity σ, placed in the dish. Simple electromagnetic field theory predicts, since there is total symmetry in the angular (ϕ) direction, that the angular component of the induced electric field, E_ϕ, varies, with radius, r, as:

$$E_\phi(t) = -\frac{dB}{dt}\frac{r}{2} \qquad (4)$$

which states the instantaneous amplitude of the induced electric field, $E_\phi(t)$, within the area of a cylindrical target, such as a laboratory dish, penetrated by a uniform magnetic field, B, is proportional to its rate of change with time, dB/dt, and the radius, r, of the target. In other words, $E_\phi(t)$ at any point in space and time is dependent upon the rate of change of B and its spatial distribution in the target. The actual waveform of $E_\phi(t)$ depends upon dB/dt, which defines the applied frequency spectrum. For example, in the case of a clinical PRF signal, which is a sinusoidal wave, dB/dt = ωB, where $\omega = 2\pi f$ (f = frequency, typically 27.12 MHz for PRF devices in the US). Since dB/dt can be controlled, the induced electric field waveform may be chosen as a function of the electrical properties of the target (impedance, bandpass).

Equation 4 shows the electric field induced in a homogenous cylindrical target is in circular loops, i.e., is rotatory, orthogonal to the magnetic field lines. In addition, the induced E field will be greater when the magnetic field intercepts a greater cross-sectional area of the sample, i.e., maximum E field in the target depends upon target size. Peak E field and associated current density, J, at a radius of 2 cm is often utilized for dosimetry comparisons. It is also convenient to use dB/dt as a measure of the peak induced electric field, assuming identical target size, for a given EMF signal. For example a common clinical bone repair signal produces 20 G peak magnetic field

in 20 μsec. Thus dB/dt = 10^6 G/sec for which peak $E_\phi(t)$ = 1 V/m = 10 mV/cm at a radius of 2 cm in the target, a typical dose metric for EMF bone growth stimulators. Note, however, that dB/dt alone is not sufficient to evaluate as a dose metric for a specific ion binding target pathway. This will be discussed in 3.8.
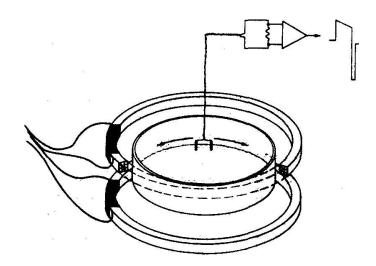

Figure 3. Schematic illustration of Helmholtz aiding coils with a plastic culture dish placed between the coils in a uniform magnetic field. This is an example of cylindrical geometry for which equation 4 is valid. A special dual electrode probe may be placed at various radii parallel to the induced electric field, allowing E_ϕ, and current density, J_ϕ, vectors to be evaluated (226). [From Pilla et al, J Biol Phys. 1983;11:51-57, with permission.

Of course, equation 4 is not valid for complex geometry and non-homogenous targets; but it is always true, from Faraday's law of induction, that the induced voltage V(t), along the line boundary of the surface S through which the flux ϕ penetrates, is:

$$V(t) = - \, d\phi(t)/dt = -d/dt \int B(t) \bullet \overline{dS}$$ **(5)**

This expression indicates that, for any geometry, the time variation of induced V will also be identical to that of E in air and any other homogeneous nonmagnetic medium contained within the boundaries defined by S.

For most PEMF clinical devices the induced electric field and associated induced currents are small enough such that back emfs (due to the magnetic field from the induced or eddy current itself) are negligible. Thus, measurements of induced fields in air accurately reflect those at the target site for the PEMF devices utilized for bone repair. On the other hand, the induced electric field from PRF devices is orders of magnitude larger at carrier frequencies between 10 and 40 MHz. Therefore, the amplitude of the incident magnetic field (in air) is always perturbed by a tissue or saline load due to the secondary field from the induced currents which act to cancel the primary magnetic field. Induced field levels and distribution have been evaluated in the presence of a tissue or saline load for PRF signals (249).

3.2 Electrochemistry at Cell Surfaces

For a living cell or tissue to respond functionally to an exogenous electric field it is necessary that it reach and be detected at the appropriate molecular, cellular or tissue site. In contrast to electrical potentials (and associated currents) which are applied directly across the cell's plasma membrane, the situation considered in this review involves the induction of electric fields within the cell/tissue target via electrical pathways originating at the external skin surface. Since cells are surrounded by a highly conducting ionic medium, it is clear that an electric field containing relatively low frequencies (< 100 MHz) can affect the cell only if current flows. This places certain constraints upon the relationship of the electrical characteristics of both the cell/tissue complex and the applied electric signal.

An important step, therefore, is the characterization of the electrical properties of cells and tissues. There are many such studies and the reader is referred to excellent reviews (231-233). However, it has also been proposed that a complete description of the electrical properties of cells and tissues should include the electrical equivalents of the electrochemical processes which could be involved in the signal transduction pathway (50). The electrical equivalents of electrochemical processes at cell surfaces and junctions and their relevance to EMF therapeutics have been described (14,15,30,49,50,234). For the purposes of this review it is simply necessary to recall that the bilayer lipid structure of the plasma membrane and the electrical double layer at its inner and outer

surfaces make the cell membrane a real capacitor, i.e., a charge storage system (240). The structure of this capacitor is determined primarily by the interactions of water dipoles and hydrated ions with the charged chemical groups associated with the various lipid, protein, and carbohydrate components of the membrane. In addition, this capacitor is leaky since transmembrane ion transport can occur. These general properties can be described using an electrochemical approach to characterize the passage of current at and across the cell membrane by combining the dielectric and electrochemical properties of the membrane. In this manner not only the passive, but also the functional electrical response of the cell/tissue target may be taken into account.

Accordingly, induced current can affect cell surfaces and junctions via a complex, but readily discernible, set of electrochemical steps which are representative of the cell's real-time response to perturbations in its charged environment for any given functional state. Impedance measurements have reported the relative magnitudes of the time constants (relaxation times) of these processes (235-238). As expected, dielectric and ion binding time constants are somewhat smaller (1-100 µsec) than those involving membrane transport (1-100 msec). In addition, the steady-state (DC) current pathway across the plasma membrane exhibits a specific resistivity several orders of magnitude above that of the extra-cellular fluid (239,241). This means exogenous EMF signals need to contain frequencies well above DC to produce detectable electric field levels in the electrochemical pathways of ion binding and/or membrane transport. Exogenous DC currents will be mostly extracellular and generally need to be significantly higher than the peak induced current density from typical PEMF therapeutic signals to affect the distribution of charges (receptors) on the cell surface via electrokinetic mechanisms (242).

The electrochemical pathways involved in the transduction of an exogenous EMF signal into a physiologically significant endpoint appear to be operationally similar to the initial gating process involved in the production of the action potential via membrane depolarization (231). It is therefore appropriate to consider the configuration of EMF waveforms in terms of an informational approach, or trigger, in contrast to one designed to supply energy to drive the biochemical cascade. Examples of the latter would be the use of direct currents large enough to cause cells to move

21

along the electric field in wound repair applications and electroporation wherein short voltage pulses are applied with sufficient electric field to temporarily cause the cell membrane to become permeable to macromolocules such as DNA or chemotherapeutic agents.

3.3 The Electrochemical Information Transfer Model

It was proposed by Pilla in 1972 that non-thermal, sub-threshold electromagnetic fields may directly affect ion binding and/or transport and possibly alter the cascade of biological processes related to tissue growth and repair (14). This electrochemical information transfer (EIT) hypothesis postulated the cell membrane as the site of interaction of low level electromagnetic fields through modulation of the rate of binding of, e.g., calcium ion to receptor sites as a first step in a biochemical cascade relevant to the desired clinical outcome.

Ionic interactions at electrically charged interfaces of a cell are generally voltage dependent (electrochemical) processes. Several distinct types of electrochemical interactions can occur at cell surfaces. One includes all of the non-specific electrostatic interactions involving water dipoles and hydrated (or partially hydrated) ions at the lipid bilayer/aqueous interface of a cell membrane which make all cell membranes a capacitor (231-233). A second involves voltage dependent ion/ligand binding. Here an ion or dipole can effectively compete with water dipoles and hydrated ions for specific membrane sites, which, in turn can modulate a downstream cascade.

Equivalent electrical circuit models representing these electrochemical processes at cell surfaces and junctions have been derived (14,15,50,234). Typically, most calculations consider a membrane model which consists of a capacitance, C_d, in parallel with an ionic leak pathway, R_M (see figure 4). While all membranes exhibit these properties, this simple model does not completely describe the dielectric properties of a functioning membrane, particularly with respect to the EMF transduction pathway. Impedance measurements on isolated cells have revealed the existence of relaxation processes which appear to reflect the kinetics of ion or ligand binding, as well as follow-up biochemical reactions (235-238). Thus, a more general description of membrane dielectric properties, which takes into account electrochemical processes relevant to EMF sensitivity,

considers an ion binding step which precedes and possibly triggers a subsequent chemical reaction at the membrane surface. The current, $i_b(\omega)$ which flows into this pathway can be written:

$$i_b(s) = q_a s \Gamma_a \Delta\Gamma_a(s) \tag{6}$$

where q_a is a coefficient representing the dependence of interfacial charge upon the surface concentration of the bound ion, Γ_a, and s ($=\sigma+j\omega$) is the complex frequency variable of the LaPlace transform (243,244). A similar analysis could, of course, be carried out for s = jω, i.e., a classical Fourier analysis (240, 243).

Equation 6 shows the current in this pathway is a function of the change in surface concentration of the binding ion with time, $\Delta\Gamma_a(s)$, which, in turn, is voltage dependent and a function of the change in surface concentration of the product of the follow-up biochemical reaction, $\Delta\beta_b(s)$. In order to derive an expression for the impedance, $Z_A(s)$, of this pathway, it is necessary to define relationships between $\Delta\Gamma_a$ and the change in transmembrane voltage (V_M), and $\Delta\beta_b(s)$. This may be written, for first order linear kinetics, as [14,234]:

$$\Delta\Gamma_a(s) = \frac{\upsilon_a}{\Gamma_a s}\left[-\Delta\Gamma_a(s) + \alpha V_M - \Delta\beta_b\right] \tag{7}$$

where υ_a is the binding rate constant and α is proportional to the potential dependence of binding ($\cong\partial\Gamma/\partial V_M$). The change in surface concentrations of the ion and the biochemical product can also be described by first order kinetics:

$$\Delta\beta_b(s) = \frac{v_b}{\beta_b s}\left[\Delta\Gamma_a(s) - \Delta\beta_b(s)\right] \tag{8}$$

where v_b is the rate constant for the follow up chemical reaction (defined as for v_a) governing the rate of formation (decomposition) of the bound biochemical product after ion binding in a molecular cleft has occurred.

Equations 6,7 and 8 allow the electrical impedance of the proposed transduction pathway at the cell membrane, $Z_A(s)$, to be written as:

$$Z_A(s) = \frac{1}{\alpha q_a} \left[\frac{1 + \Gamma_a s / v_a}{\Gamma_a s} + \frac{1}{\Gamma_a s (1 + \beta_b s / v_b)} \right] \qquad (9)$$

Inspection of equation 9 reveals the existence of two time constants, the parameters of which are identifiable in terms of the rate constant and change in surface concentration of each reaction step. Thus, the equivalent resistance of binding, R_A, is:

$$R_A = \frac{1}{\alpha q_a v_a} \qquad (10)$$

which shows the equivalent resistance of binding kinetics is, as expected, inversely proportional to the rate constant, v_a. Correspondingly, the equivalent capacitance of binding, C_A, is directly proportional to the surface concentration of the binding entity, Γ_a, as:

$$C_A = \alpha q_a \Gamma_a \qquad (11)$$

Note that the product αq_a ($\alpha \approx \partial \Gamma / \partial V_M$, $q_a = \partial q / \partial \Gamma$) in equations 10 and 11 has the dimensions of capacitance, the expected proportionality constant to enable equivalent electric circuit parameters to be related to ion binding kinetics.

The second time constant, τ_B, in equation 9 relates to the follow-up biochemical reaction:

$$\tau_B = R_B C_B = \frac{\beta_b}{v_b} \qquad (12)$$

where R_B and C_B are the equivalent resistance (inversely proportional to reaction rate, as for R_A) and capacitance (proportional to the surface concentration, β_b, of the reaction product) of the follow-up biochemical reaction, respectively. Note the follow-up reaction can be a conformational change as happens when Ca^{2+} is bound to at least three of the four available binding sites in calmodulin (288).

An electrical equivalent circuit, Z_A, which requires ion binding to occur prior to the follow-up reaction, is given in figure 4. The membrane capacitance, C_d, and leak resistance, R_M, are also shown since it is necessary to include these pathways in the total membrane impedance, Z_M, in order to fully characterize frequency dependence.
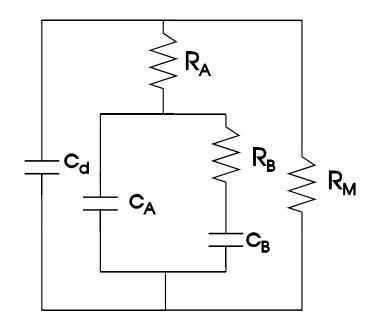
Figure 4: Electrical equivalent circuit of a cell membrane which exhibits a dielectric membrane capacitance, C_d, a leak resistance, R_M, an ion binding pathway having an equivalent resistance, R_A, and capacitance, C_A, and a time constant, $R_B C_B$, representing a coupled surface step, e.g., conformation change. This circuit requires ion binding to occur prior to the follow up step.

The impedance, $Z_d(s)$, of the C_d/R_M pathway, is given by:

$$Z_d(s) = R_M + \frac{1}{C_d s} \tag{13}$$

The most common representation of sub-excitation threshold membrane impedance is via equation 13. However, the electrochemical analysis given above shows this is not complete. Indeed, the pathways depicted in the ion binding impedance given in equation 9 have proven to be necessary to complete the EIT model. Time constants associated with electrochemical membrane processes have been reported (235-238). One model system studied was the toad urinary bladder membrane having a single cell thick epithelial layer with tight junctional electrical contact between cells, thereby affording high resolution impedance values (235). Isolated cell impedance studies utilized artificial epithelial layers created by deforming living cells under physiologic hydrostatic pressure

into well defined polycarbonate membrane filters. This technique was applied to melanoma, fibroblast, and osteoblast cells (238). In all cases the results showed, as expected, a first time constant or relaxation process due to the ubiquitous dielectric capacitance of the lipid-protein bilayer. The time constant for this process is similar for all mammalian cells, in the 1-10 µs range. However, all cells exhibited at least a second time constant which was characteristic of an ion binding pathway. The time constant for this pathway was significantly different for each cell type, ranging from 20 µs for human erythrocytes to 200 µs for fibroblasts and osteoblasts. In addition, a longer time constant was often present related to passive ion transport across the cell membrane which could be coupled to the ion binding step (50,234).

The above summarizes the EIT model which strongly guided the creation of the first clinically effective PEMF signal for recalcitrant fracture repair (51,52). According to the EIT model, the requirements for an effective waveform could be met if it contained frequency components of sufficient amplitude within the time constant of the proposed target pathway (14,15,50). Transmembrane ion transport, for which kinetics is in the millisecond range (235) was chosen as the target pathway for bone repair. This, coupled with practical restrictions on the size of the coil for patient use, led to the pulse burst waveform shown in figure 2, top. It was supposed that the cell would ignore the short opposite polarity pulse and respond only to the envelope of the burst which had a duration of 5 msec, enough to induce sufficient amplitude in the kHz frequency range. Although the reasoning behind the asymmetric pulse in this waveform was erroneous because the EIT model was not yet complete, requiring a thermal noise analysis as will become apparent below, this signal is nonetheless effective for bone repair. It continues to be part of the standard armamentarium of the orthopedist for the non-surgical non-invasive treatment of recalcitrant bone fractures.

It is important to note that the role of ions as transducers of information in the regulation of cell structure and function gained widespread acceptance well after the introduction of the EIT model. Ionic regulation mechanisms have now been described in: growth factor activation of the Na-K ATPase enzyme in fibroblasts (246,250); Ca^{2+} regulation, via CaM, of the cell cycle (251,252);

differential Ca^{2+} requirements of neoplastic vs non-neoplastic cells (245,253); Ca^{2+} dependent adenylate cyclase activation in macrophages (251). Ca/CaM regulation of growth factor and other cytokine release (247,248,254,255). EMF could also modulate the distribution of protein and lipid domains in the membrane bilayer, as well as conformational changes in lipid-protein associations by altering the kinetics of binding. Ion/ligand binding represents a coupling or transduction mechanism for exogenous electromagnetic fields at biological surfaces and junctions, which can be used to quantitatively and predictively configure bioeffective EMF waveforms.

3.4 Magnetic Field Effects

As stated previously, the first PEMF signals utilized for tissue growth and repair were configured assuming the induced electric field was the source of the stimulus (information). There is ample evidence that electric field is the dose metric for in situ PEMF signals such as those depicted in figure 2. One study showed PEMF enhanced cellular proliferation and extracellular matrix synthesis for bovine articular chondrocytes only when a pair of Helmholtz aiding coils were horizontal to the culture dish. There was no effect when the same coils inducing the same pulsing magnetic field were oriented vertical to the culture dish (262). Although the magnetic field was exactly the same for both coil orientations, the maximum electric field within the culture dish was more than a factor of ten lower for vertical vs horizontal coils, as expected from Faraday's law of induction (equation 5). This, because the height of the medium in a typical culture dish is approximately 2 mm vs a dish diameter of 35-60 mm. (Refer to figure 3 for a schematic illustration of the horizontal coil configuration.) When coils are oriented vertically current flow is at right angles to that shown in figure 3 and the path is limited to liquid height, not dish diameter.

Liburdy (263) used specially constructed annular culture dishes of differing diameter to show that calcium transport in mitogen stimulated thymic lymphocytes scaled with the induced electric field from a 22 mT, 60 Hz time-varying magnetic field. The magnetic field was identical for each loop diameter suggesting the dose metric in this case followed equation 4, which shows induced electric field amplitude is directly proportional to the target loop radius for the cylindrical geometry of this experiment. The electric field dose metric was also demonstrated in vivo by exposure of fibular

osteotomies in the rabbit to a clinically effective pulse burst PEMF signal (see figure 2) applied via an external coil or via implanted electrodes (264). The results showed the biomechanical acceleration of bone repair depended only on the in situ electric field and not on the magnetic component produced in the external coil to inductively couple the electric field to the repair site. Another study reported optimization of induced electric field parameters from time varying magnetic fields to control bone remodeling in an avian model of disuse osteoporosis (265). Finally, a recent study reported remarkable sensitivity of neutrophil metabolism to induced electric fields as low as 1 μV/cm (266). The electric vs magnetic field dose metric was specifically addressed in this study and it was established the observed results were indeed due to the induced electric field.

In contrast to the above mentioned studies, Liboff et al. (267) reported in 1984 that human fibroblasts in culture exhibited enhanced DNA synthesis when exposed to sinusoidally varying magnetic fields over a wide range of frequencies (15 Hz to 4 kHz) and amplitudes (2-600 μT). The effect appeared to be independent of the time derivative of the magnetic field, suggesting magnetic field was the dose metric for these sinusoidal waveforms. These results were somewhat controversial because the induced electric field at frequencies in the kHz range was of the same order as that reported effective for PEMF signals in cellular and clinical studies, and could clearly have contributed to the dose metric. However, this study also reported very low frequency magnetic fields in the microTesla range could produce a similar effect on DNA synthesis. For these signals the induced electric field was well below that of the clinically effective PEMF signals, suggesting a direct magnetic field effect. Thus began the ion cyclotron and parametric resonance era. These models are covered in detail elsewhere in this volume (374), however a short summary will be useful background.

Ion cyclotron resonance (ICR) (19,268-269), described frequency specific combinations of DC and AC magnetic fields which can increase ion mobility near receptor sites and/or through ion channels. The Lorentz force equation was used to relate individual influences of both AC and DC magnetic fields to ligand receptor binding and motions of ions or other charged molecules (268-270). The main objection to ICR is thermal noise (23,24,214,216,271). Bianco and Chiabrera (272)

have provided an elegant explanation of the inclusion of thermal noise in the Lorentz-Langevin model which clearly shows the force applied by a magnetic field on a charge moving outside the binding site is negligible compared to background Brownian motion and therefore has no significant effect on binding or transport at a cell surface or junction.

Because of thermal noise problems in the ICR model Lednev (20) and others (21,22,26,276-278) formulated an ion parametric resonance (IPR) quantum approach which modeled the ion in the binding site of a macromolecule (e.g., CaM) as a charged harmonic oscillator. It was proposed the presence of a static magnetic field could split the energy level of the bound ion into two sublevels with amplitudes corresponding to electromagnetic frequencies in the infrared band. The difference between these two energy levels is the Larmor frequency (= cyclotron frequency/2). The IPR model, as for the ICR model, requires parallel ac and dc magnetic fields, and that they both be present.

In addition to difficulties with the experimental verification of the IPR model (279,350-1), the main fundamental objection to the IPR model relates to excited state lifetime for the low frequency EMF signals involved (280,281). Indeed, the acceleration of the bound ion oscillating at frequencies of the order of 10^{12} Hz, obviously can not be affected by the negligible perturbations of the ion orbit generated by weak magnetic fields at 10^{10} lower frequencies. Therefore, the transition rate to the ground state cannot be affected by ELF fields and IPR can not occur (282). However, the axis of vibration of bound ligands can be affected by weak ELF, as well as DC, magnetic fields in a classical manner, e.g., Larmor precession, and some orientations may cause enhanced biological effects (23,24,28,30,213,282).

Not withstanding all of the above, a clinical device was created on the basis of the ICR model which is in current use for recalcitrant bone fractures. Clinical results from this device appear to be equivalent to those from other inductive and capacitive coupled devices (31,59,68). The signal is applied using an external pair of coils oriented parallel to one another. The alternating 40 μT sinusoidal magnetic field is at 76.6 Hz (a combination of Ca^{2+} and Mg^{2+} resonance frequencies).

The static (DC) parallel magnetic field is at 20 µT. Since there are no published clinical studies with either the AC or DC component of the magnetic field alone, there is no solid evidence that this combination of AC and DC fields is unique, or, e.g., that either the AC or DC component alone would not have produced the same clinical results. The fact remains, however, that a clinical device which produces an electrical field too weak to be detected by the tissue target has demonstrated clinical success. This can only have been achieved via a magnetic, not electric, field.

There is enough additional significant evidence showing both low frequency sinusoidal magnetic fields, which induce electric fields well below the thermal noise threshold, and weak static magnetic fields, for which there is no induced electric field, can have biologically and clinically significant effects (84-92,202-209,273,283). In these cases also, the stimulus must clearly be the magnetic field. This was unexpected, particularly for weak DC magnetic fields. There is, however, a promising, and largely overlooked, model, remarkably unhindered by thermal noise, which considers the Lorentz force on a moving charge in a binding site in terms of Larmor precession and its possible effect on reactivity (24,28,210-216). The Larmor precession model (LPM) is summarized below.

3.5 The Larmor Precession Model

Larmor precession, which describes the effects of exogenous magnetic fields on the dynamics of one state of ion binding, ions already bound, has been suggested as a possible mechanism for observed bioeffects due to weak static and alternating magnetic field exposures (210-216,271,288). A bound ionic oscillator in a static magnetic field will precess at the Larmor frequency in the plane perpendicular to the applied field. This motion will persist in superposition with thermal forces, until thermal forces eventually eject the oscillator from a binding site. For a magnetic field oriented along the z-axis, the precessional motion will be confined to the x-y plane. The LPM proposes that the biochemical reactivity of a bound ion complex may be affected by changes in the spatial orientation of the bound ionic oscillator.

The effect of weak DC and AC magnetic fields according to the LPM can be summarized as

follows. The Lorentz-Langevin equation written to describe the motion of an ion bound in a potential well (molecular cleft) subject to a magnetic field oriented along the z axis in the presence of thermal noise forces is:

$$\frac{d^2\mathbf{r}}{dt^2} = -\beta\frac{d\mathbf{r}}{dt} + \gamma\frac{d\mathbf{r}}{dt} \times B_0\mathbf{k} - \omega^2\mathbf{r} + \mathbf{n} \qquad (14)$$

where $\mathbf{r}$ is the position vector of the ion; β is the viscous damping coefficient per unit mass (due to molecular collisions in the thermal bath), γ is the ion charge to mass ratio; B_o is the magnitude of the magnetic field vector; $\mathbf{k}$ is the unit vector along the z-axis; ω is the angular frequency of the oscillator and $\mathbf{n}$ is the random thermal noise force per unit mass (271,288). It has also been shown that precession is not limited to the case of a linear isotropic oscillator potential but will occur for any central restorative potential (211).

Equation 14 describes the motion of an oscillator (ion) in a molecular cleft due to an exogenous magnetic field in the presence of thermal noise. The solution may be written (212):

$$r(t) \rightarrow e^{i\omega t}r(t) = e^{i\omega t}[C(t) + \Psi(t)] \qquad (15)$$

where r(t) is the position vector of the bound ion; C(t) is the coherent oscillation of the bound oscillator and Ψ(t) is the contribution due to thermal noise forces. The ion trajectory thus consists of a coherent part, given by:

$$C(t) = -\frac{C_0}{\omega} e^{-\frac{\beta}{2}t} e^{-i\omega_L t} \sin(\omega t) \qquad (16)$$

where C_0 is determined by initial conditions and ω_L (= $\gamma B/2$) is the Larmor frequency; and a component due to thermal noise:

$$\psi_n(t) = \frac{k_o}{\lambda_2 - \lambda_1} e^{-\frac{\beta}{2}t} e^{-\frac{i\omega_L}{2}t}[N(t)] \qquad (17)$$

where k_o is determined by initial conditions; N(t) is the accumulation of the thermal component with time; and λ_1 and λ_2 are the roots and contain the AC and DC magnetic field terms (212).

The thermal component Ψ(t) of the ion trajectory itself thus consists of an harmonic oscillator driven by thermal noise, subject to viscous damping and undergoing precessional motion at the

31

Larmor frequency about the axis defined by the magnetic field. It oscillates at the fundamental frequency of the oscillator potential with amplitude increasing over time, ultimately resulting in ejection from the binding site after a bound lifetime determined by the magnitude of thermal forces.

Both the coherent and thermal components of an ion at a binding site exhibit Larmor precession in the presence of an applied magnetic field. As the amplitude of the thermal component grows the oscillator orientation still precesses at the Larmor frequency in the plane perpendicular to the applied magnetic field direction. This is illustrated in figure 5 which shows the manner in which the amplitude of the oscillator vibration (at infrared frequencies) is affected by thermal noise. Note that, even though thermal noise is progressively adding to the amplitude of oscillator vibration, the bound ion continues to precess at the original Larmor frequency until ejected from the binding site. Thus, precession frequency is unaffected by thermal noise while the oscillator is bound. The threshold for LPM is, therefore, determined only by the bound lifetime of the charged oscillator, allowing extremely weak magnetic fields to affect its dynamics.

Although thermal forces will in general be distributed throughout the spherical solid angle available in the binding site, it is important to bear in mind that the bound ion or ligand is not executing random motions in an isotropic region. Rather, it is strongly bound in an oscillator potential, with oscillator frequency in the infrared (211,212). It is also important to emphasize that an ion bound in a molecular cleft exhibits vibrational and rotational, but not translational, degrees of freedom (395-7). This means the bound oscillator can precess, but will not retain the ability to move in the random directions permitted in its unbound trajectory.
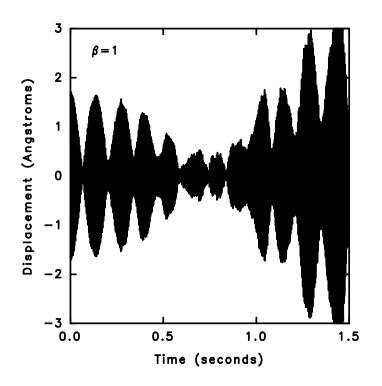
Figure 5: Overall effect of thermal white noise on precessional motion in a 10 μT static magnetic field. Note that, for this value of the viscous damping coefficient (β), precession is coherent and decays exponentially for approximately 0.5 second. Thermal noise then begins to add to the oscillator vibration amplitude, ultimately leading to ejection of the bound ion from the molecular cleft after a bound time of approximately 1.2 seconds. Until ejection, the oscillator is still precessing. [From Pilla et al., Bioelectrochem Bioenergetics. 1997;43:241-252, with permission.]

Larmor precession converts the exogenous magnetic field amplitude into a frequency determined by the gyromagnetic ratio of the target. Thus, for an ion oscillating along the z axis the Larmor frequency ω_L is:

$$\omega_L = -\Gamma B_{x,y} \qquad (18)$$

where $\Gamma = q/2m$ for a simple unhydrated ion. Equation 15 illustrates that precession frequency scales with magnetic field provided the magnetic field has components perpendicular to the axis of

33

oscillation. Note that cyclotron frequency = $2\omega_L$. Of course, the minimum detectable magnetic field is determined by the contribution of thermal energy to the bound oscillator amplitude as described above.

According to LPM, each Larmor precession frequency determines the minimum time for the bound oscillator to reach reactive orientation(s) at the binding interface. LPM predicts a bound oscillator will accelerate faster to preferred orientations in the binding site with increasing static magnetic field strength. This can increase binding rate with a resultant acceleration in the downstream biochemical cascade. According to LPM, static magnetic fields in the 0.1-1 µT range can be detected if the oscillator remains bound for the order of a second (271). To illustrate, the Larmor frequency for calcium in a 50 µT static magnetic field is approximately 18 Hz, suggesting a value for the damping coefficient, β, of about 35 or less is necessary in order for the oscillator to maintain a substantial amplitude over the period of one or more precessional orbits. The geometry of the binding site can create a locally hydrophobic region, from which dipolar molecules such as water are repelled (285), although at least one water dipole remains in a Ca/CaM binding site (287). Thus, the binding site is a region in which a bound ion would experience very few collisions, resulting in a viscosity significantly below that of bulk water, accounting for the long bound times reported for Ca/CaM.

Weak static magnetic fields have been reported to accelerate Ca/CaM dependent myosin light chain kinase (MLCK) and protein kinase C (PKC) dependent processes up to twofold (84-92,273), although one report failed to show effects in the MLCK system (274) and another, which examined Ca^{2+} binding to CaM directly using a fluorescence technique, also failed to show effects (275). Two studies reported the rate of Ca^{2+} binding to CaM was increased twofold with 2 G static magnetic field (90,92). Static magnetic fields as low as 6 G increased cell survival by reducing stress-induced apoptosis threefold via a twofold increase of Ca^{2+} influx (353). Weak DC alone (1 G) caused conformational changes in chromatin of E. coli bacteria similar in magnitude to AC/DC combinations chosen according to ICR or IPR models (354,355).

34

3.6 Resonance in the Larmor Precession Model

There are credible reports of in vitro studies which demonstrate resonance behavior for certain combinations of weak AC and DC magnetic fields (19,278,283,350,351). However, these do not unequivocally support the predictions of either the ICR or the IPR models (350). Thus, it is interesting to consider ion resonance in terms of LPM. In order to assess the combined effect of simultaneous weak AC and DC magnetic fields on Larmor precession, it is necessary to recall that the bound charged oscillator will precess when only a DC field is present according to equation 18. Addition of an AC magnetic field to an oscillator already precessing in a binding site will modulate oscillator motion for both perpendicular and parallel orientations with peak effects at multiples of the Larmor frequency.

The addition of an AC frequency in either a perpendicular or parallel direction to the axis of a precessing oscillator will modulate the axis of precession with a resultant effect on the time to reach a reactive orientation. This may be quantified by evaluation of the total excursion of the oscillator, A(t), for a given binding time, t, and for various AC/DC combinations:

$$A(t) = C_o \int_0^t \omega_L dt = \frac{C_o}{2m} \int_0^t [B_o + B_1 \cos(\omega_{AC} t)] dt = \frac{C_o}{2m} \left[B_o t + \frac{B_1}{\omega_{AC}} \sin(\omega_{AC} t) dt \right] \qquad \textbf{(19)}$$

where ω_L is the Larmor frequency; B_o is the amplitude of the DC magnetic field; B_1 and ω_{AC} are the peak amplitude and the frequency of the AC magnetic field, respectively; m is the mass of the bound oscillator; and C_o is a proportionality constant.

Equation 19 may be evaluated for any ion or ligand, any combination of AC and DC magnetic fields with any relative orientation. An example is shown in figure 6 in which DC magnetic field amplitude is varied for AC fixed at ω_L for Ca^{2+}. It may be seen that addition of an AC magnetic field to the precessing oscillator either further accelerates or inhibits its time to reach a reactive orientation. This behavior is remarkably similar to reported experimental verifications of IPR (278,351), and supports Larmor precession as a viable alternative mechanism for weak DC and AC

magnetic field bioeffects.

It is interesting to speculate whether the parameters of the AC and DC magnetic field components could be chosen to actually prohibit the bound oscillator from reaching a reactive position in the binding site. If this possibility is verified by experiment, a non-invasive treatment for pathologies such as ectopic bone formation (wherein bone grows where it should not) and malignancies without side effects could emerge.. This possibility does not appear to exist for PEMF modalities.
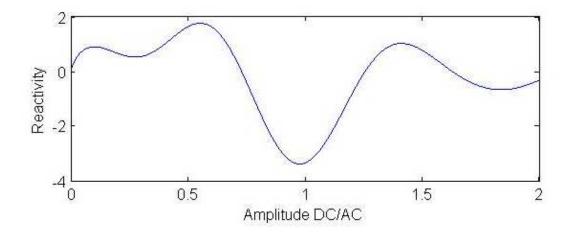

Figure 6: Effect of scanning DC magnetic field amplitude on a bound oscillator precessing at the Larmor frequency. Reactivity, e.g., Ca/CaM-dependent enzyme activity, can be either increased (vs DC field alone) or decreased, meaning addition of AC can either further accelerate or inhibit the oscillator excursion to a reactive orientation within the binding site.

3.7 The Dynamical Systems Model

Magnetic fields couple with binding kinetics via the Larmor frequency, while the induced electric field couples to the binding process via its potential dependence (see equation 7). This may be modeled by considering the binding process as a dynamical system wherein the particle has two energetically stable points separated by a few kT (double potential well), either bound in the molecular cleft, or unbound in the plane of closest approach to the hydrated surface (Helmholtz

plane) at the electrified interface between the molecular cleft and its aqueous environment (288), as shown in figure 7. Ion binding/dissociation is then treated as the process of hopping between these two states driven by thermal noise and EMF effects are measured by modulation of the ratio of time bound (in the molecular cleft) to time unbound (in the Helmholtz plane). This model does not require the ion to move in a trajectory far from the binding site, i.e., the ion is still in a prebound state while in the Helmholtz plane.

Figure 7: Cartoon of a molecular cleft illustrating an ion in a bound state which resides in the inner Helmholtz plane, IHP. Kinetics of binding is determined by ratio of time bound to unbound (outer Helmholtz plane, OHP). Bound ion hops between IHP and OHP driven by thermal noise and statistically does not drift into the diffuse double layer where it is subject to mechanical (electrokinetic) perturbation. While bound, the ion possesses rotational degrees of freedom and can precess. Note that water dipoles may remain resident in the binding site while the ion is in the bound state. [From Pilla et al., Bioelectrochem Bioenergetics. 1997; 43:241-252, with permission.]

According to this model, modulation of the kinetics of binding is considered as either a change in the height or in the bias of the energy barrier between unbound and bound states. This is thus a dynamical system wherein thermal white noise is taken as the driving force for ion binding and dissociation. The reaction coordinate $q(t)$ is subject to inertia, a damping force proportional to dq/dt and a potential energy function $V(q, E_{ind})$ dependent upon the induced electric field E_{ind}. The

37

system can be described by the following differential equation:

$$\frac{d^2q(t)}{dt^2} + \eta\frac{dq(t)}{dt} + \frac{dV(q, E_{ind})}{dq} = F_{noise} \qquad (20)$$

where η is the coefficient of damping and F_{noise} is the force due to thermal noise on the bound particle. The force imparted on a charged ion by the induced electric field may be expressed as a perturbation of the potential energy function,

$$V(q, E_{ind}) = \alpha_1\frac{q^4}{4} - \alpha_2\frac{q^2}{2} + \varepsilon q E_{ind} \qquad (21)$$

where the nonnegative coefficients α_1, and α_2, are characteristic of the receptor molecule-hydration environment and ε is the effective (hydrated) ion charge.

Equation 20 describes a double well potential wherein the potential energy wells correspond to the bound and unbound phases of the binding process. The dynamical system describes binding in a statistical sense. In terms of this model the force due to an induced electric field can modulate the relative depth of the wells thereby affecting the ratio of time bound to time unbound and thus the kinetics of the binding process. A weak magnetic field can indirectly affect the double well potential via Larmor precession by changing the dwell time of the bound vibrating oscillator, which, in turn, modulates the ratio of time bound to time unbound and therefore reaction rate.

The dynamical system model provides a rationale for linking observed static magnetic (LPM) and electric (EIT) field effects in identical molecular and cellular systems. For example, Ca^{2+}/CaM dependent myosin phosphorylation has been extensively studied with both static magnetic fields (30,90), and with several PRF signals (29). A comparison of typical results is shown in figure 8, left, which shows a 2G static field, and a 0.2G, 500μs burst of 27.12MHz sinusoidal waves at 1 burst/sec PRF signal, both accelerate phosphorylation nearly twofold in the presence of sub-optimal free Ca^{2+} concentration. Similar behavior has been obtained for dendrite outgrowth from embryonic chick ganglia in the presence of sub-optimal NGF concentration (figure 8, right). Dendrite length was also increased approximately twofold with both static and pulsing magnetic fields.

In both of these systems the PRF signal induced a time-varying electric field and negligible magnetic field (vs ambient), and the magnet produced only a static magnetic field, approximately 7X ambient. Dosimetry, therefore, depended upon the characteristics of the induced electric field for the PRF signal and on the magnetic field amplitude for the magnet. The common target pathway for both weak electric and magnetic fields, as proposed in the dynamical systems model is ion/ligand binding. The common target pathway in both cases has been proposed to be the kinetics of Ca^{2+} binding, for which signal detection (SNR) can be estimated, as shown below, for the PRF signal, or for which the Larmor precession model can be employed to makes predictions of effective, as well as saturation, static magnetic field strengths.
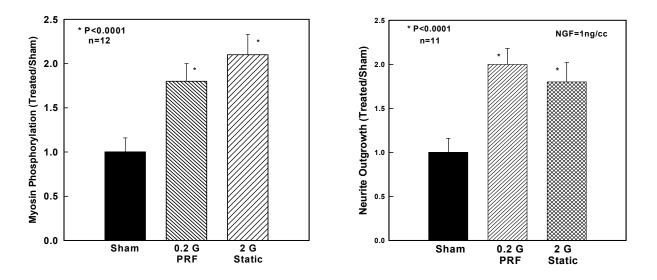

Figure 8: Comparison of the effect of a 0.2G PRF signal having a 500μs burst of 27.12 MHz sinusoidal waves repeating at 1/s, and a 2G static magnetic field on Ca^{2+}/CaM dependent myosin phosphorylation, **left**, and neurite length from embryonic chick ganglia explants, **right**. Both signals elicit the same response for identical exposure times, however, the PRF signal couples to the target pathway via induced electric field , whereas the magnet couples via magnetic field.

3.7.1 Calcium-Calmodulin Dependent Myosin Phosphorylation as a Dynamical System

Electromagnetic field effects on Ca^{2+}-calmodulin dependent myosin phosphorylation have been reported to occur only for Ca^{2+}-depleted conditions and during the nonequilibrium phase of the reaction (84-92). For these depleted conditions, enzyme kinetics favor the bound state according to

$k_{on}/k_{off} \approx 10^2$-$10^3$ (288), the instantaneous exchange reaction rate v(t) is dependent upon the instantaneous free Ca^{2+} concentration $[Ca^{2+}(t)]$, and myosin phosphorylation increases for increasing $[Ca^{2+}(t)]$. Enzyme kinetics are interpreted here in a statistical sense wherein $[Ca^{2+}(t)]$ is taken to be proportional to the ratio of the mean time the ion is free to the mean time bound:

$$[Ca^{2+}(t)] = \rho \frac{t_{free}}{t_{bound}} \tag{22}$$

where ρ is a proportionality constant.

The instantaneous exchange reaction rate v(t) for myosin phosphorylation is proportional to the concentrations of free ions and CaM, in the linear phase of the reaction and the reaction rate is thus a function of ion binding dynamics,

$$v(t) \propto [Ca^{2+} CaM] \leftrightarrow \rho \frac{t_{free}}{t_{bound}} + [CaM] \tag{23}$$

Ion binding kinetics determines the sensitivity of this system to both induced electric field and weak magnetic fields. Dosimetry for electric fields is determined by detectability in the binding pathway. This requires sufficient voltage in the binding pathway to increase net $[Ca^{2+}]$ above that due to thermal noise. The requirement is to configure the induced electric field waveform to produce sufficient amplitude in the binding pathway within the frequency range defined by binding kinetics. This will be described in detail in the next section. Direct magnetic field effects are linked via Larmor precession to ion binding kinetics. In fact, the mean residence time of Ca^{2+} in the CaM binding site must be a multiple of the binding time constant. Reported values for this time constant range between 10^{-2} and 10^{-3} sec (289). Assuming a factor of three, for simple exponential behavior, the static magnetic field effect on binding should be detectable at approximately 10 µT above ambient ($\approx$ 50 µT) and saturate at 200-300 µT. Results reported to date (90,271) support this prediction. See also figure 9.

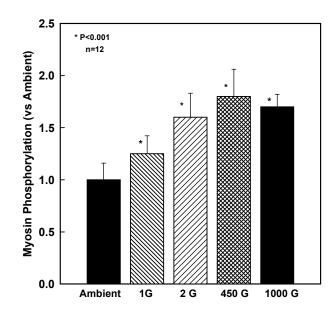**Figure 9:** Effect of static magnetic field amplitude on Ca/CaM-dependent myosin phosphorylation. Acceleration of Ca^{2+} binding appears to saturate at approximately 200 µT, as predicted by the Larmor precession model.

It should also be noted that Ca^{2+} has been implicated in the EMF transduction pathway independent of its interactions with CaM. The most commonly reported are those related to Ca^{2+} influx, efflux or oscillations (27,257-61).

3.8 Dosimetry for Induced Electric Fields

The biophysical lore prevailing until the late 1980's and lingering to this day is that, unless the amplitude and frequencies of an applied electric field were sufficient to trigger an excitable membrane (e.g. heart pacemaker), to produce tissue heating or to move an ion along a field gradient there could be no effect. This was a formidable obstacle in the quest for therapeutic applications of weak EMF signals. However, this position had to be changed as the evidence for weak (non-thermal) EMF bioeffects became overwhelming. The clinical evidence offered by many double blind clinical studies coupled with the database of hundreds of thousands of successful treatments of delayed and non-union bone fractures registered with the FDA simply could no longer be ignored. Non-invasive PEMF treatment is actually as successful as the first bone graft to

41

the huge benefit of the patient. The task now was to provide solid testable models for the biophysical mechanism of weak electric field bioeffects.

The underlying problem for any model which claims to describe the biophysical mechanism of weak EMF bioeffects relates to signal detection at the molecular/cellular/tissue target in the presence of thermal noise, i.e., signal to thermal noise ratio (SNR). Considering the cell membrane as the target, the burden of proof is to show the induced voltage is not buried in thermal and other voltage noise, i.e., that the applied signal is detectable. One of the first simple models assumed the EMF target to be a spherical cell of approximately 10 μm radius. The dielectric properties of the cell membrane in this model were limited to a simple membrane capacitance, with no attempt to take specific ion binding pathways into account. These calculations often lead to an unfavorable SNR for many EMF signals which have otherwise demonstrated biological effect (292-294). Other attempts to account for the thermal noise problem assume unsubstantiated signal processing, such as signal averaging or rectification (295), by the target pathway. Stochastic resonance in which increasing noise strength can increase SNR for a signal having frequency components at a characteristic frequency (e.g., Larmor frequency) has also been proposed (296). Finally, metabolic amplification via the out of equilibrium state of the ligand-receptor system due to basal cell metabolism has been proposed (297). None of these models have been proven experimentally.

Without resorting to signal processing or metabolic amplification, it is still necessary to attempt to understand the remarkable sensitivity of biological systems to weak electric fields. In terms of target geometry, certainly the spherical cell model is oversimplified and cannot represent the geometric complexity of cellular and tissue EMF targets. For example, the successful outcome of a healing fracture, wherein bone tissue differentiates both functionally and spatially, is a clinically relevant illustration of cell-cell communication (298). This suggests the target for the PEMF signals used to affect non-unions and delayed unions of bone is a highly organized ensemble of cells. In fact, all organized tissue is developed and maintained by an ensemble of complex geometry cells which have coordinated activity (299). The most prevalent cell shape in living system tissue is elliptical and flattened, with processes extending in at least two directions. For

example, human fibroblasts can typically exceed 100 μm when attached to a substrate (connective tissue). In addition, nerve axons can be tens of centimeters in length (364). Gap junctions provide pathways for ions and molecular intercellular communication (301). They are present in all tissues including bone. The role of cooperative organization in the EMF sensitivity of biological systems has been qualitatively considered (302). Gap junctions provide ionic coupling and metabolic cooperation, without which disorders in growth control and tissue repair, as well as neoplastic transformations, could occur (301). Functional modification of gap junctions by modulated microwave fields, as well as EMF signals has been reported (303,304). There have been several recent reports of modulation of gap junction activity by PEMF signals (305-309).

As shown in sections 3.3 and 3.4 EMF dosimetry requires knowledge of the electrical properties of the cell/tissue target. Several reports have emerged showing how induced electric field dosimetry can be altered by the presence of gap junctions (310-317,364-368). A distributed parameter electrical analog (cable) is often employed to represent the electrical properties of an ensemble of cells in gap junction contact. Most of the cable models represent the cell by a simple membrane capacitance and leak resistance (318,367,368). However proper dosimetry requires the complete electrochemical state of a functioning cell membrane to be taken into account. A summary of this approach which incorporates electrochemical processes in the electrical equivalent circuits of the cell membrane is presented below.

3.9 Cell Array Model

Gap junctions allow a group of organized cells, as in a tissue, to present a larger "antenna" to detect the induced electric field from an exogenous EMF. This increases EMF sensitivity well beyond that due to a molecule or single cell, with a resultant increase in target sensitivity. A useful model is the distributed parameter linear electrical analog (transmission line) allowing induced transmembrane voltage, V_M, to be evaluated as a function of frequency and position along the array. This is similar to the electrophysiological models which have been proposed for current spread in electrotonically coupled tissues, the DC model proposed to account for tissue sensitivity

43

to the weak electric currents commonly found in developing and regenerating tissues (314,315), for DC currents in wound repair (365) and for nonlinear electroporation (366). Obviously the complete model should be three dimensional, however the linear model presented here serves as a good first approximation to illustrate the array effect on EMF sensitivity.

The transmission line model is a lossy ladder network, or cable, of finite length, having different internal and external conductance. The "steps" of this ladder are constituted by the membrane impedance per unit length, which provides a pathway for the internal current to exit the cell. Details are available elsewhere (312), however it is useful to show how the presence of gap junctions affects the induced electric field detected in the cell array when electrochemical processes which represent the EMF transduction pathway are taken into account. The electrical equivalent circuit is shown in figure 10.
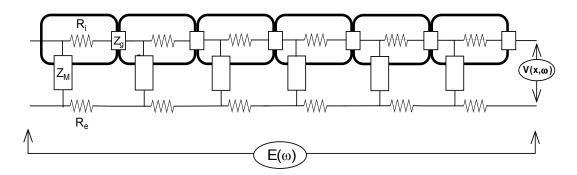

Figure 10: Distributed-parameter cell array model showing cells in gap-junction contact via impedance Z_g. This model behaves electrically identical to a transmission line wherein the applied electric field $E(\omega)$ propagates throughout the array causing progressively higher changes in induced transmembrane voltage $V(x,\omega)$. Z_M, R_i and R_e are the membrane impedance, and intracellular and extracellular resistances per unit length, respectively. Z_g represents the gap junction impedance. [From Pilla et al., Bioelectrochem Bioenergetics, 1994;35:63-69]

Induced transmembrane voltage $V_M(x,s)$ at any position x in the cable shown in figure 10 representing the cell array and for any induced electric field waveform $E(s)$ is:

$$V_M(x,s) = -E(s) \; \frac{1}{\gamma}\frac{\sinh(\gamma x)}{\cosh(\gamma L)} \tag{24}$$

44

where:

$$\gamma = \sqrt{\frac{R_e + R_i + R_g}{Z_M(s)}} \qquad (25)$$

and R_e and R_i are, respectively, the extracellular and intracellular resistances per unit length along the x axis, R_g is the gap junction resistance per unit length and $Z_M(s)$ is the membrane impedance per unit length.

Evaluation of $V_M(x,s)$ has been reported for realistic values of the specific electrical parameters related to the cell array. Typical values for R_e and R_i are $10^{10}\Omega/m$. These values would be expected to be of the same order, given the cell volume percentage for a typical tissue (50%). The values for R_g range from 10^{10} to $10^{15}\Omega/m$, representing the limiting electrical conditions of a completely open or completely closed gap junction, respectively (312). The exact form of Z_M depends upon the impedance assumed. In the most simple form a membrane consists of a capacitance, C_d, representing the real capacitor made up of the lipid bilayer and its electrified interfaces, in parallel with an ionic leak pathway, R_M, a real resistor, as discussed in section 3.4.

When an ion binding pathway is added (figure 4) the membrane admittance per unit length is:

$$Y_M(\omega) = \frac{1}{R_M} + C_d\, j\omega + \frac{1}{\left[R_A + \dfrac{1}{C_A\, j\omega} \right]} \qquad (26)$$

where R_A the equivalent binding resistance ranges between 10 to 10^3 Ω-m, and C_A the equivalent binding capacitance ranges from 10^{-6} to 10^{-5} F/m. Typical values for R_M range from 10^3 to 10^5 Ω-m, and for C_d from 10^{-7} to 10^{-6} F/m. Equation 22 describes two time constants, the first due to the membrane capacitance C_d and the membrane leak resistance R_M. The second represents the ion/ligand binding process, the parameters of which are identifiable in terms of rate constants and changes in surface concentration, as shown in section 3.3 and 3.4.

Equations 22 and 24 have been employed to evaluate the effect of signal frequency and array length, L, on induced transmembrane voltage. The example shown in figure 11, for a membrane at which

ion binding occurs, is typical of models of the effect of gap junctions or long cells on induced transmembrane voltage (310-313). As shown, there is a substantial increase in $V_M(L,\omega)$ as L increases which can render this target more sensitive to exogenous EMF signals. This is simply due to the increased size of the target. However, overall frequency response is also significantly affected. The frequency response for a single cell (L=10μm) indicates that V_M is maximum between 10^5 and 10^6 Hz, as expected. In contrast, for a 1mm cell array, V_M is about 10^2 higher than for a single cell, but only at frequencies below 100 Hz. Note the presence of the second time constant due to ion binding between 10^3 and 10^4 Hz. Interestingly, the ion binding time constant does not contribute substantially to the overall frequency response of the single isolated cell. The significance of this will become apparent below.

The presence of gap junctions in the cells of an organized or organizing (repairing) tissue cause the induced transmembrane voltage to be substantially higher than that for the same cell in isolation for the same applied EMF. The frequency range in which increased V_M occurs vs that for a single isolated cell is shifted toward a substantially lower range. This places different frequency requirements on the induced electric field waveform dependent upon whether the target is a macromolecule, single cell or tissue. As array length increases beyond 1 mm, the rate of increase in V_M diminishes because of the dissipation of intracellular current via R_M. In the case of myelinated nerve axons, R_M is substantially higher and array lengths above 1 cm can provide further significant increases in V_M (364).
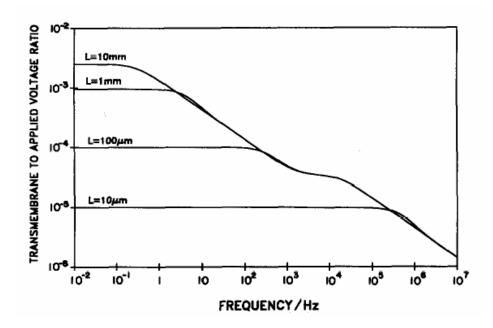
Figure 11: Frequency dependence of induced transmembrane voltage V_M for various cell array lengths. As predicted by the cell array model, there is a substantial increase in transmembrane voltage as array length L increases, but at significantly lower frequencies vs that for a single molecule or cell, reflecting the increased propagation time (low pass filter behavior) for longer array lengths.

The effect of gap junction impedance on signal amplification resulting from the cell array structure may be assessed by choosing physically meaningful values for R_g corresponding to the state of conductivity of the gap junction. When the gap junction allows macromolecules, as well as ions to pass freely, ($R_g \to 0$), its resistance is negligible compared to R_i and R_M (299). This represents a realistic lower limit for R_g. When the gap junction is completely closed, its resistance can increase to that of an insulating membrane ($R_g \to 10^{15} \Omega$/m for an artificial lipid bilayer, nearly a perfect insulator). Under these conditions, all cells in the array are still physically connected, i.e., the long antenna still exists, but has much higher DC resistance. The maximum value of R_g for a cell with a typical membrane resistance of $R_M = 10^5 \Omega$-m^2, is of the order of $10^{13} \Omega$/m.

Quantitatively, the effect of R_g is assessed using equation 24. The results are given in figure 12,

47

wherein Z_M (= $1/Y_M$) is defined by equation 26, for a 1mm array. As may be seen, signal amplification decreases as R_g increases. However, it is important to note that, even when R_g approaches the value of the membrane leak resistance (R_M), i.e., increases by a factor of 10^{13}, V_M decreases only by approximately one order. In fact, the array effect is negated, i.e., V_M is reduced to that of a single cell, only when R_g is significantly larger than the membrane leak resistance, a physiologically unrealistic limiting condition. These results strongly suggest that tissue structures, in which the cellular junctions are physically intact may always be significantly more sensitive than single cells to weak EMF, even though the resistance of the gap junction may change by several orders of magnitude throughout the functional cycles of the living cell.

Examination of equation 24 shows reasoning similar to that given above will hold for the effects of increasing intracellular resistance, R_i. It is also interesting to consider the effect of increasing transmembrane leak resistance, R_M. This is equivalent to increasing the insulating properties of the membrane, an increase of which would allow the signal to propagate a further distance along the array before substantial leakage into the extracellular compartment. An example of such an array is the nerve axon. The myelin sheath which covers the outer cell membrane surface has very high resistance which allows electrical signals to propagate tens of centimeters before the advantage of array length becomes negligible (364).
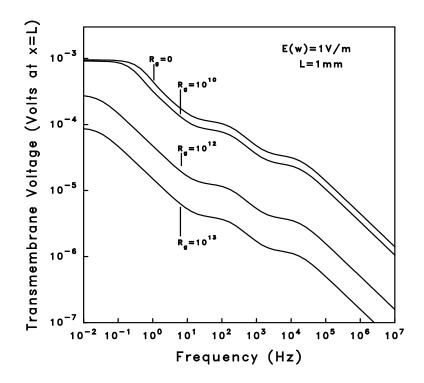
Figure 12: Effect of gap junction impedance, R_g, on spatial amplification for cells at the end of a 1mm array. An increase of many orders of magnitude in R_g has relatively little effect on the induced transmembrane voltage. When the value of R_g is equivalent to that of the transmembrane leak, a physiologically realistic limit, spatial amplification is reduced by only 10X. [From Pilla et al., Bioelectrochem Bioenergetics, 1994;35:63-69, with permission.]

The effect of gap junctions upon EMF response for cells in a culture dish has been reported (318). This study showed alkaline phosphatase activity increased in an osteosarcoma cell line only when cells were electrically connected via gap junctions. The signal employed was 30 Hz sinusoidal at 1.8 mT peak to peak amplitude. Interestingly, in the absence of gap junctions, cell division was inhibited for the same signal suggesting the magnetic component of this signal had a different biological effect. Another study (319) found that magnetic fields over a frequency range from 30 to 120 Hz and field intensities up to 12.5 G decreased gap junction intercellular communication in pre-osteoblastic cells during their proliferative phase of development in a dose dependent manner. Identical exposure conditions did not affect gap junction communication in well-differentiated osteoblastic cell line and when the pre-osteoblastic cells were more differentiated. The authors

conclude this signal may affect only less differentiated or pre-osteoblasts and not fully differentiated osteoblasts. Consequently, electromagnetic fields may aid in the repair of bone by effects exerted only on osteoprogenitor or pre-osteoblasts. This is supported by the vast clinical experience that fully differentiated and remodeled bone is not affected in a physiologically significant manner by the same EMF signal which accelerates a repairing fracture, as well as by many cellular studies. This will be reviewed in a later section.

3.10 Resonance with Electric Field Signals

As for magnetic field bioeffects, resonance is one manner by which a cellular target can have increased sensitivity to an induced electric field over a restricted frequency range. This will depend upon the structure of the membrane impedance, as can be illustrated by adding a voltage-dependent Hodgkin-Huxley K^+-conduction pathway (320-324) to the simple membrane. Because the conductance is related to the K^+ pathway resistance R_n by $g_n=1/R_n$ and the time constant τ_n has the properties of an inductance, i.e., $\tau_n=L_n/R_n$, the K^+-conduction pathway may be described via the electric circuit analog shown in figure 13. The corresponding voltage dependent admittance, $YK(V)$, written in terms of the analogous electrical circuit components for the membrane and the K^+ pathway, is thus:

$$YK(V) = \frac{1}{R_M} + i\omega C_d + \frac{g_n}{1+i\omega\tau_n} \qquad (25)$$

where g_n and τ_n are the voltage-dependent K^+ parameters given by Hodgkin and Huxley (320,321), and Fishman et. al. (321-324) and the other parameters represent the base membrane impedance.

An electric circuit analog for the K^+-conduction pathway may be formed by associating the conductance g_n with a pathway resistance R_k via $R_k=1/g_n$ and time constant τ_n to an inductance via $\tau_n=L_k/R_k$ (310). The corresponding admittance, can be written:

$$YK(V) = \frac{1}{R_M} + i\omega C_d + \frac{1}{R_k + i\omega L_k} \qquad (26)$$

The membrane model thus contains a series resistance-inductance pathway in parallel to the membrane resistance and capacitance pathway as shown in figure 13.
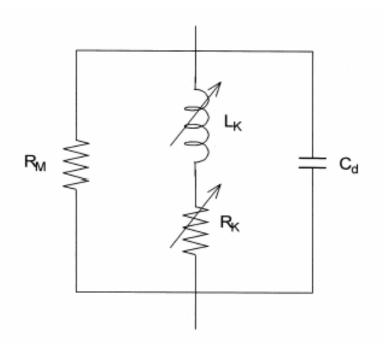
Figure 13: Potassium conductance is described in Hodgkin-Hodgkin formulation via addition of resistance-inductance branch to the simple membrane model. R_K and L_K are the equivalent voltage dependent (arrows) resistance and inductance representing the voltage dependent kinetics of K^+ transport across the cell membrane. The characteristics of the time constant $\tau_n = L_k/R_k$ of the inductive branch lead to resonance type frequency response of cell array in a low frequency range. [From Muehsam et al., Bioelectrochem Bioenergetics, 1999;48:35-42, with permission.]

The effect of the K^+ conduction membrane pathway on the frequency response of the cell array may be illustrated by holding the membrane resting potential constant (voltage clamp conditions). Using reported values for R_K and L_K in the Hodgkin–Huxley formulation, the addition of a series resistance–inductance pathway to the membrane model results in a local minimum in the admittance at low frequencies. The frequency response is shown in figure 14 wherein V_M reaches a peak at approximately 16 Hz, for a flat input ($E(\omega) = 10$ mV/cm, a typical therapeutic PEMF) and with the membrane voltage clamped at 40 mV. The introduction of a linear inductive element, according to the Hodgkin–Huxley formulation, to the membrane model produces a broad resonance response to applied fields and thus increases sensitivity to induced electric fields having frequency components in the low frequency range of this resonance. Note, however, that resonance is only significant for long cells or cells arrays, not for single cells.

51

Thus, in addition to resonances which may occur via Larmor precession for applied magnetic fields, there is also the possibility of a resonance due simply to the electrical characteristics of the target pathway. In the example given, the presence of a resonance-type response due to K^+ membrane transport depends upon the initial state of membrane polarization. The stimulus to the membrane under these conditions is well below excitatory threshold and the primary response is K^+ membrane transport for which the equivalent electric circuit contains an inductor. This, coupled with the normal capacitive properties of the cell membrane naturally leads to resonance behavior.
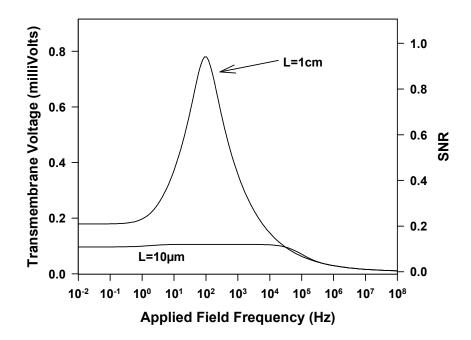

Figure 14: Response of cell array with K^+ conductance membrane model to 10 mV/cm electric field at a given transmembrane resting voltage. Frequency response of array exhibits a wide resonance response for applied field frequencies in the 16 Hz range. K^+ conductance at a given voltage is described in the Hodgkin–Huxley formulation as a series resistance–inductance branch in the membrane model. Note the broad resonance at frequencies in the 10-100 Hz range. SNR was calculated according to the method described in section 3.12. Note that resonance is not significant for a single cell, only for a long cell or cell array.

3.11 Signal to Thermal Noise

In order for an induced electric field to modulate a cellular target, the first requirement is that it be detected by the target. This means the waveform must be configured to produce sufficient

voltage at, e.g., a binding site to significantly affect the t_{free}/t_{bound} ratio for the binding ligand as defined in equation 18 (section 3.7.1). There are several sources of transmembrane noise in biological membranes. The most common are due to thermal, flicker (1/f), shot and conductance fluctuations (326). The latter three usually relate to ion transport and their interpretation is model dependent. Thermal noise is present in all voltage dependent membrane processes and represents the minimum requirement to establish adequate SNR, a front-line measure of detectability. SNR can be evaluated, assuming only the presence of thermal noise (no signal processing or other enhancements which are model dependent) via (327):

$$\text{SNR} = \frac{|V_{\text{target}}(\omega)|}{\text{RMS}_{\text{noise}}} \tag{29}$$

where $|V_{\text{target}}(\omega)|$ is the maximum amplitude of the induced voltage in the target pathway and $\text{RMS}_{\text{noise}}$ is the root mean square of the noise voltage:

$$\text{RMS}_{\text{noise}} = \left[4kT \int_{\omega_1}^{\omega_2} \text{Re}[Z_{\text{target}}(x,\omega)d\omega \right]^{1/2} \tag{30}$$

where Re represents the real part of the total impedance of the target Z_{target} and the limits of integration (ω_1, ω_2) are determined by the bandpass of the target, typically 10^{-2}-10^{7} rad/sec.

SNR, as defined above can be a powerful indicator of whether a given EMF signal can be expected to have a physiologically significant effect. To illustrate, consider a target in which the pathway is Ca/CaM-dependent. This includes most growth factors in every stage of bone and wound repair (69-83,146-7,151-3,), as well as nitric oxide synthase (NOS) which modulates NO, a signaling molecule in many neurological and cardiac pathologies and in bone and cartilage repair (328-9,390-4). To evaluate SNR for this target the quantity of interest is the effective voltage, $E_b(\omega)$ induced across the equivalent binding capacitance, C_A (see fig 4), which is directly proportional $[Ca^{2+}]$ as defined in equation 18, and given by (325):

$$E_b(\omega) = \frac{X_C \; E(\omega)}{(R_A^2 + X_C^2)^{1/2}} \tag{31}$$

where $X_C = 1/\omega C_A$ and R_A is the equivalent binding resistance. Equation 18 describes the relation between the frequency response of the target, $E_b(\omega)$, and applied field waveform $E(\omega)$,

53

illustrating clearly EMF response is dependent upon applied waveform parameters.

SNR is evaluated using $E_b(\omega)/RMS_{noise}$, however, the binding time constant $\tau_A = R_A C_A = 1/k_b$, must be known or be estimable. Consider a Ca^{2+}/CaM-dependent process, for which free $[Ca^{2+}]$ concentration is the EMF-sensitive rate-limiting factor (90,92). Linearized Michaelis-Menton kinetics describing Ca^{2+} binding to CaM is (90):

$$V_{max}/v = [1 + K_D/[Ca^{2+}]] \qquad (32)$$

where V_{max} is the maximal reaction rate, i.e. the slope of the corresponding Lineweaver-Burke plot, the reaction velocity v is given by $v = k_b [Ca^{2+}CaM]$ and K_D is the equilibrium constant.

The Michaelis-Menton relation thus determines k_b, i.e., defines the binding time constant for use in equation 27:

$$k_b = \frac{V_{max}}{[Ca^{2+}CaM](1 + K_D/[Ca^{2+}])} . \qquad (33)$$

Employing numerical values for which EMF sensitivity has been reported, $V_{max} = 10^{-6}$-10^{-7} sec^{-1}, $[Ca^{2+}] = 1$-$3\mu M$, $K_D = 20$-$40\mu M$, $[Ca^{2+}CaM] = K_D([Ca^{2+}]+[CaM])$, yields τ_A between 1-5 msec (90).

Evaluation of SNR for Ca^{2+} binding in the manner outlined above may be performed for molecular, cellular or tissue targets. An interesting example is wound repair. A common model is the full thickness linear incision performed through the skin down to the fascia on the dorsum of adult Sprague Dawley rats (331). Acceleration of wound repair is assessed by tensile strength measurements at 21 days post operative. At this time point untreated (control) strength is approximately 1/3 that of the fully healed wound. One study used the PEMF signal commonly employed for bone repair (figure 2, top) and reported no effect (332). A second, more recent study, used a PRF signal specifically configured to enhance Ca^{2+} binding to CaM with the specific goal of enhancing growth factor release and reported a 59% increase in tensile strength vs controls at 21 days, p<.001 (163,333). SNR analysis for the signals used in these studies is shown in figure 15. It is clear that the induced electric field produced by the PEMF bone repair signal, which consists of a 5 msec burst of bipolar pulses (200/20 μsec asymmetrical duration)

54

repeating at 15/sec (see figure 2, top), and inducing a gross peak electric field of 1 mV/cm (dB/dt = 10^6 G/sec), produced very low induced voltage across C_A (figure 4) in the Ca/CaM pathway. The resultant SNR was below the detectability threshold. In contrast, the PRF signal which consisted of a 2 msec burst of 27.12 MHz sinusoidal waves repeating at 1/sec, dB/dt = 10^7 G/sec, produced a significantly larger induced voltage across C_A with a larger effect on $[Ca^{2+}]$ binding. It is to be noted that increasing the gross induced electric field produced by the PEMF bone repair signal (figure 2, top) to 50 mV/cm (5X) would have increased SNR by the same factor and allowed this signal to be equally detectable in the Ca^{2+} binding target pathway. Unfortunately, such an amplitude comparison was not performed in this study.
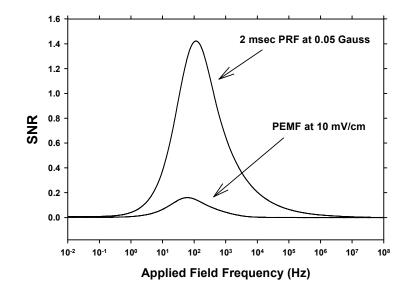

Figure 15: SNR in a Ca/CaM pathway for PEMF and PRF waveforms used in a rat cutaneous wound model. The asymmetrical repetitive pulse burst PEMF bone repair signal produced low (below detectability threshold) SNR and had no effect on wound repair. The 27.12 MHz repetitive sinusoidal burst produced sufficient SNR for detectability in the Ca/CaM pathway and enhanced tensile strength by 59% at 21 days.

A recent study compared the effects of the PEMF bone repair signal utilized in the example above (dB/dt = 10^6 G/sec) with a 65 μsec burst of rectangular pulses of 4 μsec and 12 μsec duration per polarity repeating at 1.5 bursts/sec (dB/dt = 10^4 G/sec) on bone repair in a rat osteotomy model (369). In this study the standard clinical bone repair PEMF signal produced a

twofold increase in new woven bone and callus stiffness, whereas the 4/12 μsec signal was ineffective. SNR, calculated as above for each signal, assuming a Ca/CaM target pathway, reveals peak SNR > 1 for the clinical PEMF signal and peak SNR << 1 for the 4/12 μsec signal. Note that modulation of the Ca/CaM pathway requires frequency components of sufficient amplitude in the $10^2 - 10^4$ Hz range and neither of these signals was configured accordingly.

Further support for the SNR/Dynamical Systems model for weak electric field bioeffects has been reported wherein bioeffective waveforms based upon the PRF signal were configured *a priori* for Ca/CaM-dependent myosin phosphorylation, neurite outgrowth from embryonic chick dorsal root ganglia and for bone repair in a rabbit model (29,30). Growth factor production in the latter two pathways is Ca/CaM-dependent (81,337). To illustrate signal prediction, PRF modulation of Ca/CaM-dependent myosin phosphorylation is reviewed here. Specifically, SNR was evaluated for the Ca/CaM pathway for burst durations in the 0.1-5 msec range with constant burst repetition (1/sec) and peak amplitude (0.05 G), and compared to experiment. Recall that the clinical PRF signal consists of repetitive bursts of a 27.12 MHz sinusoidal wave. SNR analysis showed peak SNR > 1 only for burst durations above 0.3 msec, with a plateau at approximately 3 msec. The experimental results shown in figure 16 suggest no significant PRF effect on myosin phosphorylation for burst durations below 0.5 msec and no further significant effect beyond approximately 4 msec, in good agreement with the SNR model.
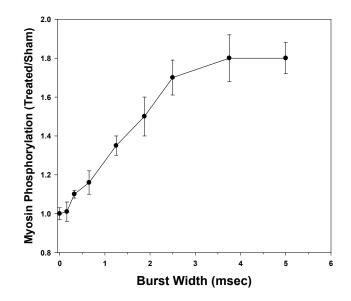
Figure 14: PRF signal modulates Ca^{2+} binding kinetics (CaM) with increased effect vs burst duration at constant amplitude (0.05 G) and repetition rate (1/sec). SNR analysis predicted a dose dependence on burst width, with a plateau at approximately 3 msec, in good agreement with experiment. The number of frequency components having detectable amplitude at the Ca^{2+} binding time constant increases with burst duration, thereby increasing SNR

4.0 ULTRASOUND FOR TISSUE REPAIR

As indicated in earlier sections, connective and endothelial tissue, particularly bone, adapt to the mechanical environment by remodeling to accommodate the magnitude and direction of the applied stress (375-6). Mechanical signals exist in functionally loaded bone (377) and represent strong regulatory signals to skeletal tissue (378), even during fracture-healing (379). Indeed, controlled movement during fracture repair has been shown to enhance healing (380). There is also considerable evidence that low intensity ultrasound (<100 mW/cm^2 SATA=Spatial Average Temporal Average) can accelerate healing of fresh fractures and established nonunions of bone (381). Indeed, US stimulation is now part of the standard armamentarium of the orthopedist. In addition, basic studies have demonstrated that ultrasound (US) can modulate each of the three key stages of the healing process (inflammation, repair, and remodeling) because it can enhance angiogenic (382), chondrogenic (383), and osteogenic (384) activity, as for PEMF signals.

57

Although it is well known that many cells have mechanoreceptors allowing direct response to a mechanical signal (385), a direct electrical effect, linking US and PEMF signals, has been proposed (199-201). The absorption of ultrasound in a tissue target gives rise to the phenomenon of micro streaming, i.e., the movement of fluid across surfaces. If the fluid contains ions and the surfaces are charged (cell membranes) streaming causes ions in the diffuse electrical double layer to be displaced from their equilibrium or resting position and the electrokinetic phenomenon of streaming potentials occurs. This could be termed a mechanically induced electrophoretic effect. US and other mechanical inputs such as controlled weight bearing during fracture repair, walking, jumping, hitting a tennis ball, etc. cause rapid flow of fluids past cell surfaces thereby generating a time-varying, mechanically induced, electric field. Should this electric field have sufficient SNR in a proposed transduction pathway, it could act in a similar manner to exogenous PEMF.

The low intensity US signal most commonly employed clinically is a 500 μsec burst of 1.5 MHz sinusoidal acoustic waves repeating at 200 Hz and at an amplitude of 30-50 mW/cm^2 SATA. The sound pressure wave causes fluid flow during each burst which, in turn, produces a repetitive time-varying voltage. This streaming potential has the form of a distorted trapezoid-like waveform with millisecond rise times and longer relaxation times, similar to the waveforms observed when bone is rapidly deformed. It has been reported that the clinical US signal produces 1-10 mV/cm peak electric field amplitude in tissue fluid (199). This waveform may be analyzed using the SNR model given above, but it is necessary to define the target pathway.

Low intensity pulsed US appears to act at the cellular level via biochemical pathways which are remarkably similar to those reported for EMF. Thus, US has been reported to induce a threefold increase in prostaglandin E2 (PGE2) production in murine osteoblasts through the upregulation of cyclooxygenase-2 (COX-2). COX-2 and PGE2 are known mediators in a bone forming response to external stimuli (386). Pulsed US induced the transient expression of the early response gene c-fos and elevated mRNA levels for insulin-like growth factor-I (IGF-I) in bone-marrow-derived stromal cells. Osteocalcin, bone sialoprotein and bone matrix proteins were also

58

modulated (387-8). US stimulation of primary rat chondrocytes elevated the intracellular concentration of Ca^{2+}. Chelating or removing Ca^{2+} from the medium inhibited the stimulatory effects of US on proteoglycan synthesis, suggesting US-stimulated synthesis of cell matrix proteoglycan, associated with accelerated fracture healing, is mediated by intracellular calcium signaling (389). US significantly increased vascular endothelial growth factor (VEGF) mRNA. Early inhibition of nitric oxide (NO) production, but not calcium or prostaglandin E2, significantly reduced US-enhanced VEGF levels. Osteoblasts responded to US treatment by increasing NO production and nitric oxide synthase (NOS) catalytic activities. Inhibition of NOS activity by N-nitro-L-arginine methyl ester (L-NAME) reduced VEGF levels (390).

The latter report is strong evidence that pulsed US acts via a pathway which is remarkably similar to that for PEMF. Indeed, PEMF has been reported to enhance proteoglycan synthesis in human cartilage cells via early stimulation of NO production (391). NO is regulated by NOS which, in turn, is activated by Ca/CaM or even by Ca^{2+} binding directly to NOS (392). This provides strong support for the validity of comparing SNR for the US and PEMF signals in the Ca^{2+} binding pathway of CaM. The results are shown in figure 17, wherein it may be seen the PEMF clinical signal (see top figure 2), as well as the streaming potential induced by the US signal, have sufficient amplitude to be detectable in the frequency range corresponding to Ca^{2+} binding kinetics.
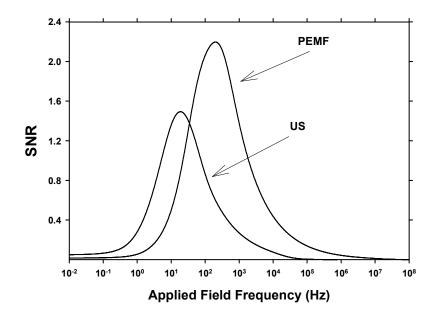
Figure 17: SNR in a Ca/CaM transduction pathway for a standard bone repair PEMF (see top, figure 2) and the streaming potential from a pulsing US signal, also in use for bone repair (see text for details). These curves show there is sufficient SNR produced by both signals in a transduction pathway which may be common to both signals. SNR peak for the US signal is shifted toward the lower frequency range reflecting the lower frequency content of the mechanically induced time-varying electric field.

This analysis may be tested by examination of results reported in the literature for the effects of PEMF and US signals on identical cellular targets. This is illustrated in figure 18 which shows both signals accelerated proteoglycan synthesis approximately twofold for chondrocytes in culture.
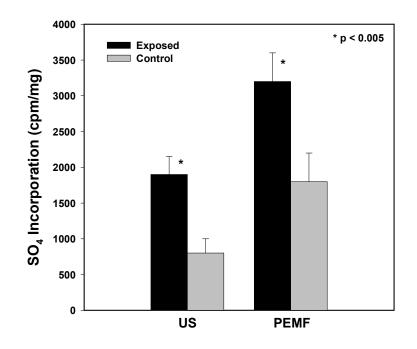
Figure 18: Comparison of the effect US and PEMF signals employed clinically for bone repair on chondrocytes in culture. Both signals accelerated proteoglycan synthesis approximately twofold suggesting the transduction pathway may be similar or even identical.

It is clear that both mechanical and EMF stimuli can modulate bone repair and affect a variety of cellular processes. The proposal that both modalities act through the EIT mechanism is reviewed here using the tools of the SNR/Dynamical systems model. This may further help the reader to assess the myriad of signals and treatment modalities reported in the rapidly expanding literature in this area.

5.0 EFFECT OF INITIAL CELL/TISSUE STATE ON EMF SENSITIVITY

Clinical experience, particularly in bone and wound repair, as well as numerous in vitro studies, suggest the initial conditions of the EMF-sensitive target pathway determine whether a physiologically meaningful bioeffect can be achieved. Thus, surrounding normal bone tissue,

61

which receives the same PEMF dose as a fracture site, does not respond in a physiologically significant manner, whereas fracture repair may be accelerated (123). Local peripheral blood flow is not affected by EMF in a healthy subject, but is increased when a musculoskeletal injury or other exogenous stimulus is present (172). Ca^{2+} binding to CaM is modulated by EMF only under depleted Ca^{2+} conditions (90). Human fibroblasts in culture exhibit maximum increase in DNA synthesis with sinusoidal EMF during the S phase of the cell cycle (267). Dendritic outgrowth in a nerve regeneration model is modulated by EMF only in the presence of sub-saturation concentrations of nerve growth factor, NGF (334-336). PEMF effects on osteoblasts depend upon their maturation stage (338).

This behavior is consistent with the SNR/Dynamical Systems model because it is known that the electrical properties of a tissue target depend upon its initial state. Indeed, SNR calculations depend upon the electrical characteristics of the EMF-sensitive target which can be substantially different when the target is at rest or when reacting to a sudden change in its environment such as a fracture or other musculoskeletal injury (339). Thus, for an identical EMF stimulus, the impedance of the EMF sensitive pathway may alter sufficiently in the presence of an injury or pathology to enable a signal, which has otherwise been ignored (not detected) to be detected.

An extension of the SNR/Dynamical System model which examines the variation of the electrical characteristics of the voltage dependent K^+ conduction model (see section 3.11) with membrane polarization has been proposed (339). Both conductance g_n and time constant τ_n (see equation 24) are voltage dependent and resting or baseline transmembrane voltage can affect membrane impedance. The electrical characteristics of the target pathway can depend upon the membrane resting potential, which, in turn, is defined by the baseline activity of the cell via, e.g., up and down regulation of receptors involved in the biochemical cascades relevant to baseline activity or response to injury.

The voltage-dependent characteristics of the Hodgkin-Huxley K^+ conduction conductance g_n and time constant τ_n produce the dependence of admittance upon membrane resting potential and

frequency shown in figure 19, left hand plot. For this example, the Hodgkin–Huxley values for the K^+ conduction pathway are employed and the time constant τ_n reaches a maximum at a membrane resting potential of about 12 mV, corresponding to the K^+ activation voltage. The admittance drops rapidly with increasing frequency, reaching its lowest value at ≈ 100 Hz.

Figure 19, right hand plot, shows the response to a flat input, $E(\omega) = 10$ mV/cm, of a 1 mm (50–100 cells) cell-array is determined by the membrane resting voltage. In a manner similar to that shown in figure 13 for the fixed-voltage K^+ pathway, the voltage-dependent K^+ pathway also exhibits a resonance like response to applied field frequencies in the 16 Hz range. However, the width of the resonance frequency region changes with changing membrane resting potential. For membrane resting voltages less than approximately -10 mV, the array responds equally to all frequencies below approximately 16 Hz. The admittance approaches zero for the depolarized membrane, so that for this condition the response of the K^+ pathway is identical to that of the simple membrane (R_M, C_d). Thus, as the membrane resting potential increases to 40 mV or more, the array (target) begins to exhibit a preferential response, producing sufficient SNR only for applied field frequencies in the 16 Hz range.
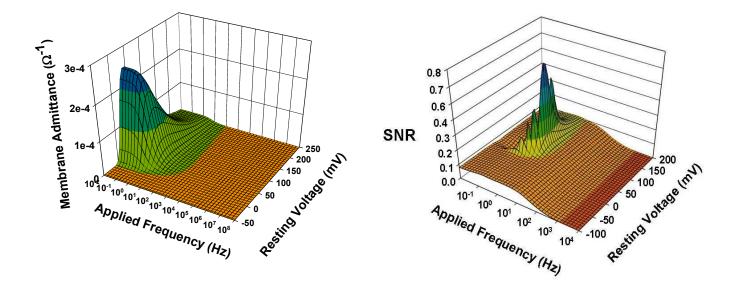
Figure 19: Left, membrane admittance depends upon frequency and membrane potential for Hodgkin-Huxley K+-conduction pathway. Region of higher admittance (reduced impedance) corresponds to greater K^+ flux across membrane and admittance drops rapidly with increasing frequency. **Right**, response of Hodgkin-Huxley K^+ conduction membrane pathway to exogenous electric field. Voltage induced in K^+ pathway varies with membrane potential and frequency. Thus, EMF sensitivity depends upon the target initial state**.**

An in vitro example of the effect of cell initial conditions upon EMF sensitivity is shown in figure 20, courtesy G. Nindl (340). Jurkat cells were exposed to the PEMF signal shown in figure 2, top. The results show the PEMF signal could only achieve sufficient SNR to produce physiologically significant results in growth stage II. Cells in early and late log growth phase were insensitive to the identical PEMF signal. The authors also report PEMF amplified the anti-proliferative effects of anti-CD3 (antibody to the T cell receptor). This was interpreted as a potential clinically significant anti-inflammatory property stemming from PEMF down-regulation of T cells that are activated at the T cell receptor during inflammation. In the absence of inflammation T cell receptors are most likely not upregulated, i.e., not EMF-sensitive and the

64

identical PEMF signal could not achieve sufficient SNR to be detected in this pathway. In terms of the cell array model this translates to a substantially different electrical impedance at this pathway, dependent upon whether the T cell receptor is up or down regulated.
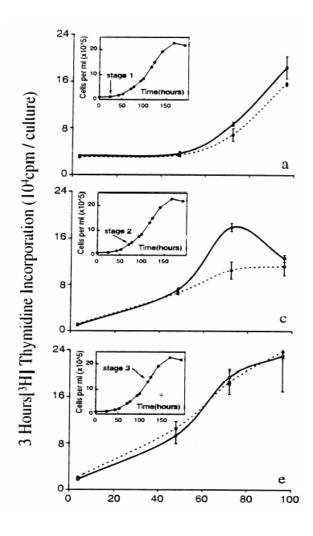

Figure 20: Illustration of the effect of cell growth stage (initial condition) upon EMF sensitivity. This study was performed on a lymphocyte cell line (Jurkat) and clearly demonstrates how an identical signal can have a large or no effect dependent upon the initial state of the cell. The authors (50) interpreted these results as down regulation, by EMF, of the T cell receptor which is apparently not up regulated in growth stages 1 or 3. [From Nindl et al. FEBS Letters 1997;414:501-506, with permission.]

It may thus been seen the complete dosimetry picture for weak EMF modulation of tissue growth and repair clearly involves the changing electrical properties of the target with functional state. Realization of this may provide an explanation for the sometimes elusive repeatability of EMF studies.

THE FUTURE

This review has attempted to provide the reader with enough information to show there is an abundance of experimental and clinical data demonstrating that exogenous electromagnetic fields of surprisingly low levels can have a profound effect on a large variety of biological systems. Both Electrical and electromagnetic devices have been demonstrated to positively affect the healing process in fresh fractures, delayed and nonunions, osteotomies, and spine fusion in orthopedics and for chronic and acute wound repair. These clinical results have been validated by well-designed and statistically powered double blind clinical trials and have survived meta analyses. The FDA has approved labeling for these biophysical devices, limited at present to these indications. EMF stimulation technologies provide an additional arm to current treatment management strategies for these pathologies. However, the potential clinical applications of EMF therapeutics extend far beyond those considered here and the clinical rewards are certain to be huge. Great strides have been made in the use of PEMF for chronic and acute wound repair. It is often the only effective treatment for chronic wounds and has been chosen as the treatment of choice for post operative pain and edema reduction in plastic and reconstructive surgery. The advent of new more effective signals may even expand applications in bone repair. There is a significant emerging application for the treatment of osteoarthritis (61,357-359) and rheumatoid arthritis (370-1).

The state of knowledge in EMF therapeutics has significantly advanced in the past decade. The mechanism of action is much better understood. So much so it is often possible to configure, *a priori*, pulsing waveforms for an expected bioeffect. The example is PEMF and PRF signals have been successfully configured for a Ca/CaM ion binding transduction pathway which the biologists have established as a primary regulatory pathway. As we continue to learn to properly match

66

dosimetry to pathology the dreams that many of us had more than 35 years ago may well be realized. Cancer, cardiac muscle regeneration, diabetes, arthritis and neurological disorders are just some of the pathologies which have already been shown to be responsive to EMF therapy. Successful applications of low-frequency electromagnetic fields have been reported for treatment of bronchial asthma, myocardial infarction and venous and varicose ulcers. There is emerging research on EMF effects on angiogenesis and the manner in which this may increase stem cell survival in the treatment of Altzeimer's and Parkinson's diseases. There are also many studies which point to the possibility of the use of EMF for peripheral nerve regeneration (334-7).

There are numerous reports suggesting a role for EMF in the treatment of cancer. In 1979-81 Larry Norton studied the effect of PEMF (using a 50 msec burst version of the PEMF signal in figure 2, top) on transplanted tumors in mice. Initial results suggested PEMF significantly increased survival time and led to preliminary clinical trials (342,343). More recent studies have continued and the basic and animal data are strong and certainly suggest human clinical applications are not far in the future (344-349,352,353,356).

EMF therapy modalities are simple, safe and significantly less costly to the health care system. They offer the ability to treat the underlying pathology rather than simply the symptoms. The time is particularly opportune given the increased incidence of side effects from the use of pharmacological agents. EMF therapeutics will have a profound impact upon health and wellness and their costs worldwide.

REFERENCES

1. Sluka KA, Walsh D. Transcutaneous Electrical Nerve Stimulation: Basic Science Mechanisms and Clinical Effectiveness. J Pain 2003; 4:109-121.
2. Rushton DN, Electrical stimulation in the treatment of pain. Disability Rehab 2002;24:407-415.
3. Bjordal JM, Johnson MI, Ljunggreen AE. Transcutaneous electrical nerve stimulation (TENS) can reduce postoperative analgesic consumption. A meta-analysis with assessment of optimal treatment parameters for postoperative pain. European J Pain 2003;7:181-188.
4. Ojingwa JC, Isseroff RR. Electrical stimulation of wound healing. J Invest Derm 2003;121:1-12.
5. Gardner SE, Frantz RA, Schmidt FL. Effect of electrical stimulation on chronic wound healing: a meta-analysis. Wound Rep Regen 1999;7:495-503.
6. Benz R, Beckers F, Zimmermann U. Reversible electrical breakdown of lipid bilayer membranes: A charge-pulse relaxation study, J. Membr. Biol., 48 (1979) 181-204.
7. Zimmermann U, Vienken J, Pilwat G. Development of drug carrier systems: electrical field induced effects in cell membranes. Bioelectrochem Bioenerg. 1980;7:553-574.
8. Mir LM. Therapeutic perspectives of in vivo cell electropermeabilization. Bioelectrochemistry. 2001;53:1-10.
9. Ferguson M, Byrnes C, Sun L, Marti G, Bonde P, Duncan M, Harmon JW. Wound healing enhancement: electroporation to address a classic problem of military medicine. World J Surg. 2005;29 Suppl 1:S55-9.
10. Gothelf A, Mir LM, Gehl J. Electrochemotherapy: results of cancer treatment using enhanced delivery of bleomycin by electroporation. Cancer Treat Rev. 2003;29:371-87.
11. Lin JC. Studies on microwaves in medicine and biology: From snails to humans. Bioelectromagnetics 2004;25:146-159.
12. Akai M, Hayashi K. Effect of electrical stimulation on musculoskeletal systems: A meta-analysis of controlled clinical trials. Bioelectromagnetics. 2002;23:132–143.
13. Akai M, Kawashima N, Kimura T, et al. Electrical stimulation as an adjunct to spinal fusion: A meta-analysis of controlled clinical trials. Bioelectromagnetics. 2002;23:496–504.
14. Pilla AA - Electrochemical information and energy transfer in vivo. Proc. 7th IECEC, Washington, D.C., American Chemical Society, 1972; 761-64.
15. Pilla A.A. Electrochemical Information Transfer at Living Cell Membranes. Ann NY Acad Sci, 1974;238:149-170.
16. Chiabrera A, Grattarola M, Viviani R. Interaction between electromagnetic fields and cells: microelectrophoretic effect of ligands and surface receptors. Bioelectromagnetics 1984;5:173-178.
17. McLeod BR, Liboff AR. Dynamic characteristics of membrane ions in multifield configurations of low-frequency electromagnetic radiation. Bioelectromagnetics 1986;7:177-189.
18. Chiabrera A, Bianco B. The role of the magnetic field in the EM interaction with ligand binding. In: Mechanistic Approaches to Interactions of Electric and Electromagnetic Fields with Living Systems. M Blank, E Findl (eds), Plenum Press, NY 1987, pp. 79-90.
19. Liboff AF, Fozek RJ, Sherman ML, McLeod BR, Smith SD. Ca^{2+}-45 cyclotron resonance in human lymphocytes. J Bioelectricity 1987;6:13–22.
20. Lednev VV. Possible mechanism for the influence of weak magnetic fields on biological systems. Bioelectromagnetics 1991;12:71-75.
21. Blanchard JP, Blackman CF. Clarification and application of an ion parametric resonance model for magnetic field interactions with biological systems. Bioelectromagnetics 1994;15:217–238.
22. Engstrom S. Dynamic properties of Lednev's parametric resonance mechanism. Bioelectromagnetics 1996;17:58-70
23. Muehsam DS, Pilla AA. Lorentz approach to static magnetic field effects on bound ion dynamics and binding kinetics: thermal noise considerations, Bioelectromagnetics 1996;17:89-99.
24. Zhadin MN. Combined action of static and alternating magnetic fields on ion motion in a macromolecule: Theoretical aspects. Bioelectromagnetics 1998;19:279-292.
25. Chiabrera A, Bianco B, Moggia E, Kaufman JJ. Zeeman-Stark modeling of the RF EMF interaction with ligand binding. Bioelectromagnetics 2000;21:312-324.
26. Binhi VN. Amplitude and frequency dissociation spectra of ion-protein complexes rotating in magnetic fields. Bioelectromagnetics 2000;21:34-45.
27. McCreary CR, Thomas AW, Prato FS. Factors confounding cytosolic calcium measurements in Jurkat E6.1 cells during exposure to ELF magnetic fields. Bioelectromagnetics 2002;23:315-328.
28. Zhadin M, Barnes F. Frequency and amplitude windows in the combined action of DC and low frequency AC magnetic fields on ion thermal motion in a macromolecule: Theoretical analysis. Bioelectromagnetics 2005;26:323-330.
29. Pilla AA, Muehsam DJ, Markov MS, Sisken BF. EMF signals and ion/ligand binding kinetics: Prediction of bioeffective waveform parameters.1999;48:27-34.
30. Pilla AA. Weak time-varying and static magnetic fields: From mechanisms to therapeutic applications. In: Biological Effects of Electromagnetic Fields, P. Stavroulakis, ed. Springer Verlag, 2003, pp. 34-75.
31. Ryaby JT. Clinical effects of electromagnetic and electric fields on fracture healing. Clin Orthop. 1998;355(suppl):205–215.
32. Yasuda I. Piezoelectric activity of bone. J Japanese Orthop Surg Soc. 1954;28:267-271.
33. Yasuda I, Noguchi K, Sata T. Dynamic callus and electric callus. J Bone Joint Surg Am 1955;37:1292–1293.
34. Fukada E, Yasuda I. On the piezoelectric effect of bone. J Phys Soc Japan 1957;12:121-128.
35. Becker RO. The bioelectric factors in amphibian-limb regeneration. J Bone Joint Surg. 1961;43A: 643
36. Bassett CAL. Biological significance of piezoelectricity. Calc Tiss Res. 1968;1:252-261.

37. Friedenberg ZB, Brighton CT. Bioelectric potentials in bone. J Bone Joint Surg. 1966;48A:915-923.

38. Shamos MH, Lavine LS. Piezoelectricity as a fundamental property of biological tissues. Nature 1967;212:267-268.

39. Williams WS, Perletz L. P-n junctions and the piezoelectric response of bone. Nat New Biol. 1971; 233:58-59.

40. Anderson JC, Eriksson C. Electrical properties of wet collagen. Nature 1968;227:166-168.

41. Bassett CAL, Pawluk RJ. Electrical behavior of cartilage during loading. Science 1974;814:575-577.

42. Grodzinsky AJ, Lipshitz H, Glimcher MJ.) Electromechanical properties of articular cartilage during compression and stress relaxation. Nature 1978;275:448-450.

43. Kim Y-J, Bonassar LJ, Grodzinsky AJ. The role of cartilage streaming potential, fluid flow and pressure in the stimulation of chondrocyte biosynthesis during dynamic compression. J Biomechanics 1995;28:1055-1066.

44. Spadaro JA. Electrically stimulated bone growth in animals and man. Clin Ortho. 1977;122:325-29.

45. Black J. Electrical Stimulation: Its Role in Growth, Repair, and Remodeling of the Musculoskeletal System. New York: Praeger; 1987.

46. Spadaro JA. Mechanical and electrical interactions in bone remodeling. Bioelectromagnetics 1997;18:193-202.

47. Brighton CT. The treatment of non-unions with electricity. J Bone Joint Surg. 1981;63A:8-12.

48. Friedenberg ZB, Harlow MC, and Brighton CT. Healing of non-union of the medial malleolus by means of direct current. J. Trauma 1971;11:8831.

49. Pilla AA. Electrochemical Events in Tissue Growth and Repair. In: "Electrochemical Bioscience and Bioengineering", I. Miller, A. Salkind and H. Silverman, eds., Electrochem. Society Symposium Series, Princeton, New Jersey, pp. 1-17, 1973.

50. Pilla AA. Mechanisms of Electrochemical Phenomena in Tissue Growth and Repair. Bioelectrochem Bioenergetics, 1974;1:227-243.

51. Bassett CAL, Pawluk RJ, Pilla AA. Acceleration of Fracture Repair by Electromagnetic Fields. Ann NY Acad Sci. 1974;238:242-262.

52. Basset CAL, Pilla AA, Pawluk R. A non-surgical salvage of surgically-resistant pseudoarthroses and non-unions by pulsing electromagnetic fields - Clin Orthop 1977;124:117-131.

53. Bassett C, Mitchell S, Gaston S. Treatment of ununited tibial diaphyseal fractures with pulsing electromagnetic fields. J Bone Joint Surg. 1981;63A:511–523.

54. Bassett C, Mitchell S, Schink M. Treatment of therapeutically resistant nonunions with bone grafts and pulsing electromagnetic fields. J Bone Joint Surg. 1982;64A:1214–1224.

55. Bassett C, Valdes M, Hernandez E. Modification of fracture repair with selected pulsing electromagnetic fields. J Bone Joint Surg. 1982;64A:888–895.

56. Mooney, V. A randomized double blind prospective study of the efficacy of pulsed electromagnetic fields for interbody lumbar fusions. Spine. 1990;15:708-715.

57. Goodwin, C.B., Brighton, C.T., Guyer, R.D., Johnson, J.R., Light, K.I., and Yuan, H.A. (1999) A double blind study of capacitively coupled electrical stimulation as an adjunct to lumbar spinal fusions. Spine 24, 1349-1357.

58. Zdeblick, T.D. (1993) A prospective, randomized study of lumbar fusion: preliminary results. Spine 18, 983-991.

59. Linovitz, R.J., Ryaby, J.T., Magee, F.P., Faden, J.S., Ponder, R., and Muenz, L.R. (2000) Combined magnetic fields accelerate primary spine fusion: a double-blind, randomized, placebo controlled study. Proc. Am. Acad. Orthop. Surg. 67, 376.

60. Nicolakis P, Kollmitzer J, Crevenna1 R, Bittner C, Erdogmus CB, Nicolakis J. Pulsed magnetic field therapy for osteoarthritis of the knee – a double-blind sham-controlled trial. Wien Klin Wochenschr. 2002;16:678–684.

61. Zizic T, Hoffman P, Holt D, Hungerford J, O'Dell J, Jacobs M, et al. The treatment of osteoarthritis of the knee with pulsed electrical stimulation. J Rheumatol. 1995;22:1757-61.

62. Mont MA, Hungerford DS, Caldwell JR, Hoffman KC, He YD, Jones LC, Zizic TM. The use of pulsed electrical stimulation to defer total knee arthroplasty in patients with Osteoarthritis of the knee. American Academy of Orthopaedic Surgeons. Mar, 2004

63. Aaron RK, Lennox D, Bunce GE, Ebert T. The conservative treatment of osteonecrosis of the femoral head. A comparison of core decompression and pulsing electromagnetic fields. Clin Orthop. 1989;249:209-218.

64. Steinberg ME, Brighton CT, Corces A, Hayken GD, Steinberg DR, Strafford B, Tooze SE, Fallon M. Osteonecrosis of the femoral head. Results of core decompression and grafting with and without electrical stimulation. Clin Orthop. 1989;249:199-208.

65. Binder, A., Parr, G., Hazelman, B., and Fitton-Jackson, S. (1984) Pulsed electromagnetic field therapy of persistent rotator cuff tendinitis: a double blind controlled assessment. Lancet 1(8379), 695-697.

66. Brighton C, Pollack S. Treatment of recalcitrant non-unions with a capacitively coupled electrical field. J Bone Joint Surg. 1985;67A:577–585.

67. Brighton CT, Hozack WJ, Brager MD, Windsor RE, Pollack SR, Vreslovic EJ, Kotwick JE. Fracture healing in the rabbit fibula when subjected to various capacitively coupled electrical fields. J Orthop Res. 1985;3:331-340.

68. Aaron RK, Ciombor DMcK, Simon BJ. Treatment of Nonunions With Electric and Electromagnetic Fields. Clin Orthop. 2004;419:21–29.

69. Fitzsimmons RJ, Ryaby JT, Magee FP, Baylink DJ. Combined magnetic fields increase net calcium flux in bone cells. Calcif Tiss Intl. 1994;55:376-380.

70. Fitzsimmons RJ, Baylink DJ, Ryaby JT, Magee FP. EMF-stimulated bone cell proliferation, in Electricity and Magnetism in Biology and Medicine (M.J. Blank, ed.) San Francisco Press, San Francisco, 1993, pp. 899-902.

71. Fitzsimmons RJ, Ryaby JT, Mohan S, Magee FP, Baylink DJ. Combined magnetic fields increase IGF-II in TE-85 human bone cell cultures. Endocrinology 1995;136:3100-3106.

72. Fitzsimmons RJ, Ryaby JT, Magee FP, Baylink DJ. IGF II receptor number is increased in TE 85 cells by low amplitude, low frequency combined magnetic field (CMF) exposure. J Bone Min Res. 1995;10:812-819.

73. Ryaby JT, Fitzsimmons RJ, Khin NA, Culley PL, Magee FP, Weinstein AM, Baylink DJ.) The role of insulin-like growth factor in magnetic field regulation of bone formation. Bioelectrochem Bioenergetics. 1994;35:87-91.

74. Aaron RK, Ciombor D McK, Jones AR. Bone induction by decalcified bone matrix and mRNA of TGFb and IGF-1 are increased by ELF field stimulation. Trans Orthop Res Soc. 1997;22:548.

75. Ciombor McKD. Lester G, Aaron RK, Neame P, Caterson B: Low frequency EMF regulates chondrocyte differentiation and expression of matrix proteins. J Orthop Res. 2002;20:40–50.

76. Aaron RK, Ciombor DMcK. Acceleration of experimental endochondral ossification by biophysical stimulation of the progenitor cell pool. J Orthop Res 1996;14:582-589.

77. Aaron RK, Ciombor DMcK, Jolly G. Stimulation of experimental endochondral ossification by low-energy pulsing electromagnetic fields. J Bone Min Res. 1989;4:227-233.

78. Lohmann CH, Schwartz Z, Liu Y, Guerkov H, Dean DD, Simon B, Boyan BD. Pulsed electromagnetic field stimulation of MG63 osteoblast-like cells affects differentiation and local factor production. J Orthop Res. 2000;18:637-646.

79. Guerkov HH, Lohmann CH, Liu Y, Dean DD, Simon BJ, Heckman JD, Schwartz Z, Boyan BD. Pulsed electromagnetic fields increase growth factor release by nonunion cells. Clin Orthop. 2001;384:265-279.

80. Zhuang H, Wang W, Seldes RM, Tahernia AD, Fan H, Brighton CT. Electrical Stimulation induces the level of TGF-beta1 mRNA in osteoblastic cells by a mechanism involving calcium/calmodulin pathway, Biochem Biophys Res Commun, 1997;237:225-229.

81. Brighton CT, Wang W, Seldes R, Zhang G, Pollack SR. Signal Transduction in Electrically Stimulated Bone Cells. J Bone Joint Surg. 2001;83-A:1514-1523.

82. Bodamyali T, Bhatt B, Hughes FJ, Winrow VR, Kanczler JM, Simon B, Abbott J, Blake DR, Stevens CR. Pulsed electromagnetic fields simultaneously induce osteogenesis and upregulate transcription of bone morphogenetic proteins 2 and 4 in rat osteoblasts in vitro. Biochem. Biophys. Res. Commun. 1998;250:458-61.

83. Aaron RK, Boyan BD, Ciombor DMcK, Schwartz Z, Simon BJ. Stimulation of Growth Factor Synthesis by Electric and Electromagnetic Fields. Clin Orthop 2004;419:30–37.

84. Markov MS, Ryaby JT, Kaufman JJ, and Pilla AA - Extremely weak AC and DC magnetic field significantly affect myosin phosphorylation - in Charge and Field Effects in Biosystems-3, M.J.Allen, S.F.Cleary, A.E.Sowers, D.D.Shillady (eds.) Birkhauser, Boston 1992; 225-230

85. Markov MS, Wang S, and Pilla AA - Effects of weak low frequency sinusoidal and DC magnetic fields on myosin phosphorylation in a cell-free preparation - Bioelectrochemistry and Bioenergetics 30 (1993) 119-125

86. Markov MS, Pilla AA - Ambient range sinusoidal and DC magnetic fields affect myosin phosphorylation in a cell-free preparation - in Electricity and Magnetism in Biology and medicine, M Blank (ed), San Francisco Press 1993: 323-327

87. Markov MS, Pilla AA. Static Magnetic Field Modulation of Myosin Phosphorylation: Calcium Dependence in Two Enzyme Preparations. Bioelectrochemistry and Bioenergetics 1994;35:57-61.

88. Markov MS, Pilla AA. Modulation of Cell-Free Myosin Light Chain Phosphorylation with Weak Low Frequency and Static Magnetic Fields, in "On the Nature of Electromagnetic Field Interactions with Biological Systems", Fry, AH, ed., R.G. Landes Co., Austin, 1994, pp. 127-141.

89. Markov MS, Muehsam DJ, Pilla AA. Modulation of Cell-Free Myosin Phosphorylation with Pulsed Radio Frequency Electromagnetic Fields, in "Charge and Field Effects in Biosystems 4", Allen MJ, Cleary SF, Sowers AE, eds, World Scientific, New Jersey, 1994, pp. 274-288.

90. Markov MS, Pilla AA: Weak Static Magnetic Field Modulation of Myosin Phosphorylation in a Cell-Free Preparation: Calcium Dependence, Bioelectrochemistry and Bioenergetics, 43 (1997) 235-240.

91. Engstrom S, Markov MS, McLean MJ, Holcomb RR, Markov JM. Effects of non-uniform static magnetic fields on the rate of myosin phosphorylation. Bioelectromagnetics 2002;23:475-479.

92. Liboff AR Cherng S, Jenrow KA, Bull A. Calmodulin-dependent cyclic nucleotide phosphodiesterase activity is altered by 20 mT magnetostatic fields. Bioelectromagnetics 2003;24:32-38.

93. Yen-Patton GP, Patton WF, Beer DM, et al. Endothelial cell response to pulsed electromagnetic fields: stimulation of growth rate and angiogenesis in vitro. J Cell Physiol 1988;134:37-39.

94. Tepper OM, Callaghan MJ, Chang EI, Galiano RD, Bhatt KA, Baharestani S, Gan J, Simon B, Hopper RA, Levine JP, Gurtner GC. Electromagnetic fields increase in vitro and in vivo angiogenesis through endothelial release of FGF-2. FASEB J. 2004;18:1231-3.

95. Bassett CAL, Pawluk RJ, Pilla AA. Acceleration of Fracture Repair by Electromagnetic Fields. Ann NY Acad Sci. 1974;238:242-262.

96. Bassett CAL, Pawluk RJ, Pilla AA. Augmentation of Bone Repair by Inductively Coupled Electromagnetic Fields. Science, 1974;184:575-578.

97. Cane V, Botti P, Farnetti P, Soana S. Electromagnetic stimulation of bone repair: a histomorphometric study. J Orthop Res. 1991;9: 908-917.

98. Cane V, Botti P, Soana S. Pulsed magnetic fields improve osteoblast activity during the repair of an experimental osseous defect. J Orthop Res. 1993;11:664-670.

99. Brighton CT, Katz MJ, Goll SR, Nichols CE, Pollack SR. Prevention and treatment of sciatic denervation disuse osteoporosis in the rat tibia with capacitively coupled electrical stimulation. Bone 1985;6:87 97.

100. Brighton CT, Luessenhop CP, Pollack SR, Steinberg DR, Petrik ME, Kaplan FS.) Treatment of castration induced osteoporosis by a capacitively coupled electrical signal in rat vertebrae. J Bone Joint Surg. 1989;71A:228-236.

101. Skerry TM, Pead MJ, Lanyon LE. Modulation of bone loss during disuse by pulsed electromagnetic fields. J Orthop Res. 1991;9:600-608.

102. Ryaby JT, Haupt DL, Kinney JH. Reversal of osteopenia in ovariectomized rats with combined magnetic fields as assessed by x-ray tomographic microscopy. J Bone Min Res. 1996;11:S231.

103. McLeod KJ, Rubin CT. The effect of low-frequency electrical fields on osteogenesis. J Bone Joint Surg. 1992;74A:920-929.

104. Connolly J, Ortiz J, Price R, et al. The effect of electrical stimulation on the biophysical properties of fracture healing. Ann N Y Acad Sci. 1974;238:519–529.

105. Petersson C, Holmar N, Johnell O. Electrical stimulation of osteogenesis: Studies of the cathode effect on rat femur. Acta Orthop Scand. 1982;53:727–732.
106. Bassett C, Valdes M, Hernandez E. Modification of fracture repair with selected pulsing electromagnetic fields. J Bone Joint Surg. 1982;64A:888–895.
107. Inoue N, Ohnishi I, Chen D, et al. Effect of pulsed electromagnetic fields (PEMF) on late-phase osteotomy gap healing in a canine tibial model. J Orthop Res. 2002;20:1106–1114.
108. France JC, Norman TL, Santrock RD, et al. The efficacy of direct current stimulation for lumbar intertransverse process fusions in an animal model. Spine. 2001;26:1002–1008.
109. Nerubay J, Marganit B, Bubis JJ, et al. Stimulation of bone formation by electrical current on spinal fusion. Spine. 1986;11:167–169.
110. Toth JM, Seim HB, Schwardt JD, et al. Direct current electrical stimulation increases the fusion rate of spinal fusion cages. Spine. 2000;25:2580–2587.
111. Dejardin LM, Kahanovitz N, Arnoczky SP, et al. The effect of varied electrical current densities on lumbar spinal fusions in dogs. Spine. 2001;1:341–347.
112. Inoue N, Ohnishi I, Chen D, Deitz LW, Schwardt JD, Chao EY. Effect of pulsed electromagnetic fields (PEMF) on late-phase osteotomy gap healing in a canine tibial model. J Orthop Res. 2002;20:1106-14.
113. Fini M, Cadossi R, Cane V, Cavani F, Giavaresi G, Krajewski A, Martini L, Aldini NN, Ravaglioli A, Rimondini L, Torricelli P, Giardino R. The effect of pulsed electromagnetic fields on the osteointegration of hydroxyapatite implants in cancellous bone: a morphologic and microstructural in vivo study. J Orthop Res. 2002;20:756–763
114. Smith TL, Wong-Gibbons D, Maultsby J. Microcirculatory effects of pulsed electromagnetic fields. J Orthop Res. 2004;22:80-4.
115. Borsalino G, Bagnacani M, Bettati E, et al. Electrical stimulation of human femoral intertrochanteric osteotomies. Clin Orthop. 1988;237:256–263.
116. Mammi GI, Rocchi R, Cadossi R, et al. The electrical stimulation of tibial osteotomies: A double-blind study. Clin Orthop. 1993;288:246–253.
117. Traina G, Sollazzo V, Massari L. Electrical Stimulation of Tibial Osteotomies: A Double Blind Study. In: Bersani F (ed). Electricity and Magnetism in Biology and Medicine. New York: Kluwer Academic/Plenum; 1999:137–138.
118. Kahanovitz N. Electrical stimulation of spinal fusion: A scientific and clinical update. Spine. 2002;2:145–150.
119. Oishi M, Onesti S. Electrical bone graft stimulation for spinal fusion: A review. Neurosurgery. 2000;47:1041–1056.
120. Rogozinski A, Rogozinski C. Efficacy of implanted bone growth stimulation in instrumented lumbosacral spinal fusion. Spine. 1996;21:2479–2483.
121. Meril AJ. Direct current stimulation of allograft in anterior and posterior lumbar interbody fusions. Spine. 1994;19:2393–2398.
122. Goodwin CB, Brighton CT, Guyer RD, et al. A double-blind study of capacitively coupled electrical stimulation as an adjunct to lumbar spinal fusions. Spine. 1999;24:1349–1356.
123. Gossling HR, Bernstein RA, Abbott J. Treatment of ununited tibial fractures: A comparison of surgery and pulsed electromagnetic fields (PEMF). Orthopedics. 1992;15:711–719.
124. Paterson D, Lewis G, Cass C. Treatment of delayed union and nonunion with an implanted direct current stimulator. Clin Orthop. 1980;148:117–128.
125. Brighton C, Black J, Friedenberg Z. A multicenter study of the treatment of non-union with constant direct current. J Bone Joint Surg. 1981;63A:2–13.
126. Bassett C, Mitchell S, Gaston S. Treatment of ununited tibial diaphyseal fractures with pulsing electromagnetic fields. J Bone Joint Surg. 1981;63A:511–523.
127. Heckman J, Ingram A, Loyd R. Nonunion treatment with pulsed electromagnetic fields. Clin Orthop. 1981;161:58–66.
128. Bassett C, Mitchell S, Schink M. Treatment of therapeutically resistant nonunions with bone grafts and pulsing electromagnetic fields. J Bone Joint Surg. 1982;64A:1214–1224.
129. Brighton C, Pollack S. Treatment of recalcitrant non-unions with a capacitively coupled electrical field. J Bone Joint Surg. 1985;67A:577–585.
130. Sedel L, Christel P, Duriez J, Duriez R, Evrard J, Ficat C, Cauchoix J, Witvoet J. Acceleration of repair of non-unions by electromagnetic fields. Rev Chir Orthop Reparatrice Appar Mot. 1981;67:11-23.
131. DeHaas W, Watson J, Morrison D. Noninvasive treatment of ununited fractures of the tibia using electrical stimulation. J Bone Joint Surg. 1980;62B:465–470.
132. Dunn AW, Rush GA. Electrical stimulation in treatment of delayed union and nonunion of fractures and osteotomies. South Med J. 1984;77:1530–1534.
133. Sharrard W. A double blind trial of pulsed electromagnetic fields for delayed union of tibial fractures. J Bone Joint Surg. 1990;72B:347–355.
134. Scott G, King J. A prospective double blind trial of electrical capacitive coupling in the treatment of non-union of long bones. J Bone Joint Surg. 1994;76A:820–826.
135. Brighton C, Shaman P, Heppenstall R. Tibial nonunion treated with direct current, capacitive coupling, or bone graft. Clin Orthop. 1995;321:223–234.
136. Fredericks DC, Piehl DJ, Baker JT, Abbott J, Nepola JV. Effects of pulsed electromagnetic field stimulation on distraction osteogenesis in the rabbit tibial leg lengthening model. J Pediatr Orthop. 2003;23:478-83.
137. Wysocki AB. Wound fluids and the pathogenesis of chronic wounds. J Wound Ostomy Care Nurs. 1996;23:283–290.
138. CMS. Decision memo for electrostimulation for wounds (CAG-00068R), 2003. http://www.cms.hhs.gov/mcd/
139. Burr HS, Taffel M, Harvey SC. Electrometric study of the healing wound in man. Yale J Biol Med. 1940;12:483–485.
140. Burrows H, Iball J, Roe EMF. Electrical changes in wounds and inflamed tissues: Part 1. The bioelectric potentials of cutaneous wounds in rats. Br J Exp Pathol 1942;23:253-257.
141. Barnes TC. Healing rate of human skin determined by measurement of the electrical potential of experimental abrasions. Am J Surg. 1945;69:82–88.
142. Barker AT. Measurement of direct current in biological fluids. Med Biol Eng Comput 1981;19:507–8.
143. Barker AT, Jaffe LF, Vanable JW Jr. The glabrous epidermis of cavies contains a powerful battery. Am J Physiol 1982;242:R358–R366.
144. Foulds IS, Barker AT. Human skin battery potentials and their possible role in wound healing. Br J Dermatol 1983;109:515–22.
145. Iglesia DD, Vanable, JW. Endogenous lateral electric fields around bovine corneal lesions are necessary for and can enhance normal rates of wound healing. Wound Rep Reg. 1998; 6:531-542.

146. Fang KS, Farboud B, Nuccitelli R, Isseroff RR. Migration of human keratinocytes in electric fields requires growth factors and extracellular calcium. J Invest Dermatol. 1998; 111:751–756.

147. Lee RC, Canaday DJ, Doong H. A review of the biophysical basis for the clinical application of electric fields in soft-tissue repair. J Burn Care Rehabil 1993; 14:319-335.

148. Carley PJ, Wainapel SF. Electrotherapy for acceleration of wound healing: low intensity direct current. Arch Phys Med Rehabil 1985; 66:443-446.

149. Gentzkow GD. Electrical stimulation to heal dermal wounds. J Dermatol Surg Oncol 1993; 19:753-758.

150. Vodovnik L, Miklavcic D, Sersa G. Modified cell proliferation due to electrical currents. Med Biol Eng Comput 1992; 30:CE21-28.

151. Goodman E, Greenebaum B, Frederiksen J. Effect of pulsed magnetic fields on human umbilical endothelial vein cells. Bioelectrochemistry and Bioenergetics 1993; 32:125-132.

152. Amaral SL, Linderman JR, Morse MM, Greene AS. Angiogenesis induced by electrical stimulation is mediated by angiotensin II and VEGF. Microcirculation 2001; 8:57-67.

153. Greenough CG. The effects of pulsed electromagnetic fields on blood vessel growth in the rabbit ear chamber. J Orthop Res 1992; 10:256-262.

154. Nikolaev AV, Shekhter AB, Mamedov LA, Novikov AP, Manucharov NK. Use of a sinusoidal current of optimal frequency to stimulate the healing of skin wounds. Biull Eksp Biol Med 1984; 97:731-734.

155. McLeod KJ, Lee RC, Ehrlich, HP. Frequency dependence of electric field modulation of fibroblast protein synthesis. Science 1987; 236:1465-1469.

156. Katsir G, Baram SC, Parola AH. Effect of sinusoidally varying magnetic fields on cell proliferation and adenosine deaminase specific activity. Bioelectromagnetics 1998; 19:46-52.

157. Supino R, Bottone MG, Pellicciari C, Caserini C, Bottiroli G, Belleri M, Veicsteinas A. Sinusoidal 50 Hz magnetic fields do not affect structural morphology and proliferation of human cells in vitro. Histol Histopathol 2001;16:719-726.

158. George FR, Lukas RJ, Moffett J, Ritz MC. In-vitro mechanisms of cell proliferation induction: A novel bioactive treatment for accelerating wound healing. Wounds 2002; 14:107-115.

159. Gilbert TL, Griffin N, Moffett J, Ritz MC, George FR. The Provant Wound Closure System induces activation of p44/42 MAP kinase in normal cultured human fibroblasts. Ann N Y Acad Sci 2002; 961:168-171.

160. Cho MR, Marler JP, Thatte HS, Golan DE. Control of calcium entry in human fibroblasts by frequency-dependent electrical stimulation. Front Biosci 2002;7:1-8.

161. Roland, D, Ferder M, Kothuru R, Faierman T, Strauch B. Effects of pulsed magnetic energy on a microsurgically transferred vessel. Plast Reconstr Surg. 2000;105:1371-1374.

162. Weber RV, Navarro A, Wu JK, Yu HL, Strauch B. Pulsed magnetic fields applied to a transferred arterial loop support the rat groin composite flap. Plast Reconstr Surg 2004;114:1185-1189.

163. Strauch B, Patel MK, Navarro A, Berdischevsky M, Pilla AA. Pulsed magnetic fields accelerate wound repair in a cutaneous wound model in the rat. Plast Reconstr Surg. 2005.

164. Glassman LS, McGrath MH, Bassett CA. Effect of external pulsing electromagnetic fields on the healing of soft tissue. Ann Plast Surg 1986; 16:287-295.

165. Ginsberg AJ. Ultrashort radiowaves as a therapeutic agent. Med Record 1934;140:651-653.

166. Salzberg CA, Cooper SA, Perez P, Viehbeck MG, Byrne DW. The effects of non-thermal pulsed electromagnetic energy on wound healing of pressure ulcers in spinal cord-injured patients: a randomized, double-blind study. Ostomy Wound Management 1995;41:42-51.

167. Kloth LC, Berman JE, Sutton CH, Jeutter DC, Pilla AA, Epner ME. Effect of Pulsed Radio Frequency Stimulation on Wound Healing: A Double-Blind Pilot Clinical Study, in "Electricity and Magnetism in Biology and Medicine", Bersani F, ed, Plenum, New York, 1999, pp. 875-878.

168. Pilla AA, Martin DE, Schuett AM, et al. Effect of pulsed radiofrequency therapy on edema from grades I and II ankle sprains: a placebo controlled, randomized, multi-site, double-blind clinical study. J Athl Train. 1996;S31:53.

169. Pennington GM, Danley DL, Sumko MH, et al. Pulsed, non-thermal, high frequency electromagnetic energy (Diapulse) in the treatment of grade I and grade II ankle sprains. Military Med. 1993;158:101-104.

170. Foley-Nolan D, Barry C, Coughlan RJ, O'Connor P, Roden D. Pulsed high frequency (27MHz) electromagnetic therapy for persistent neck pain: a double blind placebo-controlled study of 20 patients. Orthopedics 1990;13:445-451.

171. Foley-Nolan D, Moore K, Codd M, et al. Low energy high frequency pulsed electromagnetic therapy for acute whiplash injuries: a double blind randomized controlled study. Scan J Rehab Med. 1992;24:51-59.

172. Mayrovitz HN, Larsen PB. Effects of Pulsed Magnetic Fields on Skin Microvascular Blood Perfusion. Wounds: A Compendium of Clinical Research and Practice 1992;4:192-202.

173. Mayrovitz HN, Larsen PB. A Preliminary Study to Evaluate the Effect of Pulsed Radio Frequency Field Treatment on Lower Extremity Peri-Ulcer Skin Microcirculation of Diabetic Patients. Wounds: A Compendium of Clinical Research and Practice 1995;7:90-93.

174. Mayrovitz HN, Macdonald J, Sims N. Effects of pulsed radio frequency diathermy on postmastectomy arm lymphedema and skin blood flow: A pilot investigation. Lymphology 2002.

175. Kenkre JE, Hobbs FD, Carter YH, Holder RL, Holmes EP. A randomized controlled trial of electromagnetic therapy in the primary care management of venous leg ulceration. Fam Pract 1996; 13:236-241.

176. Musaev AV, Guseinova SG, Imamverdieva SS. Application of impulse complex modulated electromagnetic fields in management of patients with diabetic polyneuropathy. Zh Nevrol Psikhiatr Im S S Korsakova. 2002;102:17-24.

177. Goldin JH, Broadbent NRG, Nancarrow JD, Marshall T. The effects of Diapulse on the healing of wounds: a double-blind randomized controlled trial in man. Br J Plast Surg. 1981;34:267-270.

178. Itoh M, Montemayor JS, Jr., Matsumoto E, Eason A, Lee MH, Folk FS. Accelerated wound healing of pressure ulcers by pulsed high peak power electromagnetic energy (Diapulse). Decubitus 1991; 4:24-25, 29-34.

179. Seaborne D, Quirion-DeGirardi C, Rousseau M. The treatment of pressure sores using pulsed electromagnetic energy (PEME). Physiotherapy Canada 1996; 48:131-137.

180. Comorosan S, Vasilco R, Arghiropol M, Paslaru L, Jieanu V, Stelea S. The effect of diapulse therapy on the healing of decubitus ulcer. Rom J Physiol 1993; 30:41-45.

181. Ieran M, Zaffuto S, Bagnacani M, Annovi M, Moratti A, Cadossi R. Effect of low frequency electromagnetic fields on skin ulcers of venous origin in humans: a double blind study. J Orthop Res. 1990;8:276-282.

182. Stiller MJ, Pak GH, Shupack JL, Thaler S, Kenny C, Jondreau L. A portable pulsed electromagnetic field (PEMF) device to enhance healing of recalcitrant venous ulcers: a double-blind, placebo- controlled clinical trial. Br J Dermatol 1992; 127:147-154.

183. Canedo-Dorantes L, Garcia-Cantu R, Barrera R, Mendez-Ramirez I, Navarro VH, Serrano G. Healing of chronic arterial and venous leg ulcers with systemic electromagnetic fields. Arch Med Res 2002; 33:281-289.

184. Bentall RHC. Low-level pulsed radiofrequency fields and the treatment of soft-tissue injuries. Bioelectricity and Bioenergetics 1986; 16:531-548.

185. Maddin WS, Bell PW, James JHM. (1990) The biologic effects of a pulsed electrostatic field with specific reference to hair. Int J Dermatol 29:446–450.

186. Maddin WS, Amara I, Sollecito WA. (1992) Electrotrichogenesis: Further evidence of efficacy and safety on extended use. Int J Dematol 31:878–880.

187. Benjamin B, Ziginskas D, Harman J, Meakin T. (2002) Pulsed Electrostatic Fields (ETG) to Reduce Hair Loss in Women Undergoing Chemotherapy for Breast Carcinoma: A Pilot Study. Psycho-Oncology 11:244–248.

188. Trock DH, Bollet AJ, Markoll R. The effect of pulsed electromagnetic fields in the treatment of osteoarthritis of the knee and cervical spine. Reports of randomized, double blind, placebo controlled trials, J Rheumatol. 1994;21:1903–1911.

189. Trock DH, Bollet AJ, Dyer RH, Fielding LP, Miner WK, Markoll R. A double-blind trial of the clinical effects of pulsed electromagnetic fields in osteoarthritis, J Rheumatol. 1993;20:456–460.

190. Dyson M, Brookes M. Stimulation of bone repair by ultrasound. Ultrasound Med Biol. 1983;8:61-66.

191. Duarte LR. The stimulation of bone growth by ultrasound. Arch Orthop Trauma Surg. 1983;101:153-159.

192. Pilla AA, Mont MA, Nasser PR, Khan SA, Figueiredo M, Kaufman JJ, Siffert RS. Non-invasive low-intensity pulsed ultrasound accelerates bone healing in the rabbit. J Orthop Trauma 1990;4:246-253.

193. Pilla AA, Figueiredo M, Nasser P, Alves JM, Ryaby JT, Klein M, Kaufman JJ, Siffert RS, Kristiansen T, Heckman J. Acceleration of bone repair by pulsed sine wave ultrasound: Animal, clinical, and mechanistic studies. In "Electromagnetics in Biology and Medicine" (Brighton, C.T. and Pollack, S.R., eds.), San Francisco Press, San Francisco, (1991) pp. 331-341.

194. Tis JE, Meffert CR, Inoue N, McCarthy EF, Machen MS, McHale KA, Chao EY. The effect of low intensity pulsed ultrasound applied to rabbit tibiae during the consolidation phase of distraction osteogenesis. J Orthop Res. 2002;20:793-800.

195. Chang WH-S, Sun J-S, Chang S-P, Lin JC. Study of Thermal Effects of Ultrasound Stimulation on Fracture Healing. Bioelectromagnetics 2002;23:256-263.

196. Heckman JD, Ryaby JP, McCabe J, Frey JJ, Kilcoyne RF. Acceleration of tibial fracture-healing by non-invasive, low-intensity pulsed ultrasound. J. Bone Joint Surg. 1994;76A:26-34.

197. Kristiansen TK, Ryaby JP, McCabe J, Frey JJ, Roe LR. Accelerated healing of distal radial fractures with the use of specific, low-intensity ultrasound. A multicenter, prospective, randomized, double-blind, placebo-controlled study. J. Bone Joint Surg. 1997;79A:961-973.

198. Rubin CT, Bolander M. Ryaby JP, Hadjiargyrou M. The use of low-intensity ultrasound to accelerate the healing of fractures. J. Bone Joint Surg. 2001;83A:259-270.

199. Pilla AA, Nasser PR. A unified mechanoelectric approach to Wolff's Law for streaming potentials and exogenous EMF, Trans Orthopaedic Research Soc. 1993;18:151.

200. Pilla AA, Muehsam DJ, Nasser PR. A unified mechanoelectric basis for bone repair and remodelling via streaming potentials as the primary cellular messenger. Trans Orthopaedic Research Soc. 1995;20:589.

201. Pilla AA. Low-intensity electromagnetic and mechanical modulation of bone growth and repair: are they equivalent? J Orthop Sci 2002;7:420–428.

202. Valbona C, Hazlewood CF, Jurida G. Response of pain to static magnetic fields in post-polio patients: A double-blind pilot study. Arch Phys Med Rehabil. 1997;78:1200-1207.

203. Man D, Man B, Plosker H. The influence of permanent magnetic field therapy on wound healing in suction lipectomy patients: A double-blind study. Plastic Reconst Surg. 1999;104:2261-2266.

204. Colbert AP, Markov MS, Banerij M, Pilla AA. Magnetic mattress mad use in patients with fibromyalgia: A randomized double-blind pilot study. J Back Musculoskeletal Rehab. 1999;13:19-31.

205. Alfano AP, Taylor AG, Foresman PA, Dunkl PR, McConnell GG, Conway MR, Gillies GT. Static magnetic fields for treatment of fibromyalgia: a randomized controlled trial. J Alternative Comp Med. 2001;7:53-64.

206. Weintraub MI. Magnetic bio-stimulation in painful diabetic peripheral neuropathy: a novel intervention – a randomized double-placebo crossover study. Am J Pain Manag. 1999;9:8-17.

207. Brown CS, Ling FW, Wan JY, Pilla AA.. Efficacy of Static Magnetic Field Therapy in Chronic Pelvic Pain: A Double-Blind Pilot Study. Am J Obs Gyn. 2002;187:1581-7.

208. Weintraub MI, Wolfe GI, Barohn RA, Cole SP, Parry GJ, Hayat G, Cohen JA, Page JC, Bromberg MB, Schwartz SL. Static magnetic field therapy for symptomatic diabetic neuropathy: A randomized, double-blind, placebo-controlled trial. Arch Phys Med Rehabil. 2003;84:736-46.

209. Wolsko PM, Eisenberg DM, Simon LS, Davis RB, Walleczek J, Mayo-Smith M, Kaptchuk TJ, Phillips RS. Double-blind placebo-controlled trial of static magnets for the treatment of osteoarthritis of the knee: results of a pilot study. Altern Ther Health Med. 2004;10:36-43.

210. Zhadin MN, Fesenko EE. Ionic cyclotron resonance in biomolecules. Biomed Sci 1990; 1:245–250.

211. Edmonds DT. Larmor precession as a mechanism for the detection of static and alternating magnetic fields. Bioelectrochem Bioenerg. 1993; 30:3-12.

212. Muehsam DJ, Pilla AA. Weak magnetic field modulation of ion dynamics in a potential well: mechanistic and thermal noise considerations. Bioelectrochem Bioenerg. 1994; 35:71-79.

213. Muehsam DS, Pilla AA. Lorentz Approach to Static Magnetic Field Effects on Bound Ion Dynamics and Binding Kinetics: Thermal Noise Considerations. Bioelectromagnetics 1996; 17:89-99.

214. Zhadin MN. Effect of magnetic fields on the motion of an ion in a macromolecule: Theoretical analysis. Biophysics 1996; 41:843–860.

215. Pilla AA, Muehsam DJ, Markov MS. A dynamical systems/Larmor precession model for weak magnetic field bioeffects: Ion-binding and orientation of bound water molecules. Bioelectrochem Bioenergetics 1997;43:239-249.

216. Zhadin MH. Combined action of static and alternating magnetic fields on ion motion in a macromolecule: theoretical aspects. Bioelectromagnetics 1998; 19:279–292.

217. Blank M, Goodman R. Do electromagnetic fields interact directly with DNA? Bioelectromagnetics. 1997;18:111-5.

218. Blank M, Goodman R. Electromagnetic fields may act directly on DNA. J Cell Biochem. 1999;75:369-74.

219. Adair RK. Extremely low frequency electromagnetic fields do not interact directly with DNA. Bioelectromagnetics. 1998;19:136-8.

220. Seegers JC, Engelbrecht CA, van Papendorp DH. Activation of signal-transduction mechanisms may underlie the therapeutic effects of an applied electric field. Medical Hypotheses 2001; 57:224–230.

221. Chiabrera A, Grattarola M, Viviani R, Braccini C. Modelling of the perturbation induced by low-frequency electromagnetic fields on the membrane receptors of stimulated human lymphocytes. Studia Biophysica 1982;90:77-81.

222. Pilla AA, Schmukler RE, Kaufman JJ and Rein G. Electromagnetic modulation of biological processes: consideration of cell-waveform interaction. In "Interactions between Electromagnetic Fields and Cells", A Chiabrera, C Nicolini and HP Schwan (eds.) Plenum Press, NY, 1985; 423-436.

223. Pilla AA, Kaufman JJ, Ryaby JT. Electrochemical kinetics at the cell membrane: A physicochemical link for electromagnetic bioeffects. In "Mechanistic Approaches to Interactions of Electric and Electromagnetic Fields with Living Systems", M. Blank and E. Findl (eds.) Plenum Press, NY, 1987; 39-62.

224. Pilla AA. State of the art in electromagnetic therapeutics. In: "Electricity and Magnetism in Biology and Medicine". M.Blank (ed.) - San Francisco Press Inc. (1993) 17-22.

225. Nelson FR, Brighton CT, Ryaby J, Simon BJ, Nielson JH, Lorich DG, Bolander M, Seelig J. Use of physical forces in bone healing. J Am Acad Orthop Surg. 2003; 11:344-54.

226. Pilla AA, Sechaud P, McLeod BR. Electrochemical and electric current aspects of low frequency electromagnetic current induction in biological systems. J Biol Phys. 1983;11:51-57.

227. McLeod BR, Pilla AA, Sampsel MW. Electromagnetic fields induced by Helmholtz aiding coils inside saline-filled boundaries. Bioelectromagnetics 1983;4:357-370.

228. Hart FX. Cell culture dosimetry for low-frequency magnetic fields. Bioelectromagnetics 1996;17:48-57.

229. van Amelsfort AMJ. An analytical algorithm for solving inhomogeneous electromagnetic boundary-value problems for a set of coaxial circular cylinders, Ph.D. Thesis, Eindhoven University, The Netherlands, 1991.

230. Buechler DN, Christensen DA, Durney CH, Simon B. Calculation of electric fields induced in the human knee by a coil applicator. Bioelectromagnetics. 2001; 22:224-31.

231. Plonsey R, Fleming DG. Bioelectric phenomena. McGraw-Hill, NY, 1969.

232. Foster KR, Schwan HP. Dielectric properties of tissues. In Critical Reviews in Biomedical Engineering, 1989; 17:25–104. New York: Begall House.

233. Gabriel, This Volume

234. Pilla AA. Electrochemical information transfer at cell surfaces and junctions: Application to the study and manipulation of cell regulation. In: "Bioelectrochemistry". Keyser H and Gutman F, eds. Plenum Press, NY, 1980, pp. 353-396.

235. Pilla AA, Margules G. Dynamic interfacial electrochemical phenomena at living cell membranes: Application to the toad urinary bladder membrane system. J Electrochem Soc. 1977;124:1697-1706.

236. Pilla AA: Membrane Impedance as a Probe for Interfacial Electrochemical Control of Living Cell Function. Adv. in Chem. A.C.S., 188:339-359, 1980.

237. Margules G, Doty SB, and Pilla AA: Impedance of Living Cell Membranes in the Presence of Chemical Tissue Fixative. Adv. in Chem., A.C.S., 188:461-484, 1980.

238. Schmukler RE, Kaufman JJ, Maccaro PC, Ryaby JT, and Pilla AA: Transient Impedance Measurements on Biological Membranes: Application to Red Blood Cells and Melanoma Cells. In "Electrical Double Layers in Biology", Blank M, ed. Plenum Press, New York, pp. 201-210, 1986.

239. Blinks LR. The direct current resistance of Nitella. J Gen Physiol. 1930; 13:495-508.

240. Cole KS, Cole RH. Dispersion and Absorption in Dielectrics I. Alternating Current Characteristics. J Chem Phys 1941; 9:341-351.

241. Kao CY. Changing electrical constants of the Fundulus egg plasma membrane. J Gen Physiol. 1956; 40:107-119.

242. Poo MM, Poo WJ, Lam JW. Lateral electrophoresis and diffusion of Concanavalin A receptors in the membrane of embryonic muscle cell. J Cell Biol. 1978; 76:483-501.

243. Cheng DK. Analysis of Linear Systems. Addison-Wesley, London, 1959

244. Pilla AA. A transient impedance technique for the study of electrode kinetics. J Electrochem Soc. 1970;117:467-477.

245. Quastel MR, Kaplan JG. Inhibition by ouabain of human lymphocyte transformation induced by phytohaemagglutinin in vitro. Nature 1968; 219:198-200.

246. Kaplan JG. Membrane cation transport and the control of proliferation of mammalian cells. Ann Rev Physiol. 1978; 40:19-41.

247. Means AR, Rasmussen CD. Calcium, calmodulin and cell proliferation. Cell Calcium. 1988; 9:313-318.

248. Berridge MJ. Calcium signal transduction and cellular control mechanisms. Biochim Biophys Acta. 2004;1742:3-7.

249. Markov MS, Pilla AA : Electromagnetic Field Stimulation of Soft Tissue: Pulsed Radio Frequency Treatment of Post-Operative Pain and Edema, Wounds 1995;7:143-151.

250. Boonstra J, Van der Sagg PT, Moolenarr WH, DeLaat SW. Rapid effects of nerve growth factor on Na+,K+-pump in rat pheochromocytoma cells. Exp Cell Res. 1981;131:452-455.

251. Whifield JF, Boyton AL, MacManus JP, Rixon RH, Sikorska M, Tsong B, Walker RP, Smierenga SH. The roles of calcium and cyclic AMP in cell proliferation. Ann NY Acad Sci. 1981;339:216-240.

252. Chafoules JC, Bolton WE, Hidaka H, Boyd AE, and Means HR. Calmodulin involvement in regulation of cell-cycle progression. Cell 1982;28:41-50.

253. Boynton AL, Whitfield JF, Isaacs RJ, Trembley RG. Different extracellular calcium requirement for proliferation of nonneoplastic, preneoplastic and neoplastic mouse cells. Cancer Res. 1977;37:2657-2661.

254. Hazelton B, Tupper J. Calcium transport and exchange in mouse 3T3 and SV40-3T3 cells. J Cell Biol. 1979;81:538-542.

255. Gemsa D, Seitz M, Kramer W, Grimm W, Till G, Resch K. Ionophore A 23187 Raises cyclic AMP levels in macrophages by stimulation prostaglandin E formation. Exp Cell Res. 1979;118:55-62.

256. Chiabrera A, Bianco B, Caratozzolo F, Gianetti G, Grattarola M, Viviani R Electric and magnetic field effects on ligand binding to the cell membrane. In Interactions between Electromagnetic Fields and Cells Chiabrera A, Nicolini C, Schwan HP, (eds) New York, Plenum Press, 1985:253

257. Lyle DB, Wang X, Ayotte RD, Sheppard AR, Adey WR - Calcium Uptake by Leukemic and Normal T Lymphocytes Exposed to Low Frequency Magnetic Fields Bioelectromagnetics 1991; 12: 145

258. Bawin SM, Kaczmarek LK, and Adey WR - Effects of modulated VHF fields on the central nervous system - Ann. NY Acad.Sci. 1975; 247: 74-91

259. Blackman CF, Benane SG, Kinney LS, Joines WT, and House DE - Effects of ELF fields on calcium efflux from brain tissue in vitro - Radiat. Res. 1982; 92: 510

260. Blackman CF, Benane SG, Rabinowitz JR, House DE, Joines WT - A role for the magnetic field in the radiation-induced efflux of Ca-ions from brain tissue in vitro -Bioelectromagnetics 1985; 6: 327

261. Wei LX, Goodman R, Henderson AS - Changes in levels of c-myc and histone H2B following exposure of cells to low-frequency sinusoidal electromagnetic fields: evidence for a window effect -Bioelectromagnetics 1990; 11: 269

262. Elliott JP, Smith RL, Block CA. Time-varying magnetic fields: effects of orientation on chondrocyte proliferation. J Orthop Res. 1988; 6:259-64.

263. Liburdy RP. Calcium signaling in lymphocytes and ELF fields: Evidence for an electric field metric and a site of ion channel interaction involving the calcium ion channel. FEBS Letters. 1992; 301:53-59.

264. Pilla AA, Figueiredo M, Nasser PR, Kaufman JJ, Siffert RS: Broadband EMF Acceleration of Bone Repair in a Rabbit Model is Independent of Magnetic Component, in, "Electricity and Magnetism in Biology and Medicine", Blank M, ed., San Francisco Press, 1993, pp. 363-367.

265. Rubin CT, Donahue HJ, Rubin JE, McLeod KJ. Optimization of electric field parameters for the control of bone remodeling: exploitation of an indigenous mechanism for the prevention of osteopenia. J Bone Miner Res. 1993; 8:573-581.

266. Rosenspire AJ, Andrei L. Kindzelskii AL, Simon BJ, Petty HJ. Real-Time control of Neutrophil metabolism by very weak ultra-low frequency pulsed magnetic fields. Biophysical Journal 2005; 88:3334–3347.

267. Liboff AR, Williams T Jr, Strong DM, Wistar R Jr. Time-varying magnetic fields: effect on DNA synthesis. Science. 1984; 223:818-820.

268. Liboff AR. Cyclotron resonance in membrane transport, in: Interactions between in Interactions Between Electromagnetic Fields and Cells, A Chiabrera, C Nicolini, HP Schwan (eds)Plenum Press, New York 1985: 281

269. Liboff AR, Smith SD, McLeod BR - Experimental evidence for ion cyclotron resonance mediation of membrane transport -In Mechanistic Approaches to Interactions of Electric and Electromagnetic Fields with Living Systems M Blank and E Findl (eds), Plenum Press, NY 1987: 109

270. Chiabrera A, Bianco B, Kaufman JJ, Pilla AA. Resonant Phenomena. In: "Interaction Mechanisms of Low Level Electromagnetic Fields in Living Systems". Stockholm: Royal Swedish Academy of Sciences, 1989: 256

271. Muehsam DJ, Pilla AA: Weak Magnetic Field Modulation of Ion Dynamics in a Potential Well: Mechanistic and Thermal Noise Considerations, Bioelectrochemistry and Bioenergetics, 35 (1994) 71-79.

272. Bianco B, Chiabrera A. From the Langevin-Lorentz to the Zeeman model of electromagnetic effects on ligand-receptor binding. Bioelectrochemistry and Bioenergetics, 1992; 28:355-365.

273. Shuvalova LA, Ostrovskaja MV, Sosunov EA, and Lednev VV - Weak magnetic field influence of the speed of calmodulin dependent phosphorylation of myosin in solution - Dokladi Acad Nauk USSR 1991; 217: 227.

274. Coulton LA, Barker AT, Van Lierop JE, Walsh MP. The effect of static magnetic fields on the rate of Calcium/Calmodulin-dependent phosphorylation of myosin light chain. Bioelectromagnetics 2000; 21:189-196.

275. Hendee SP, Faour FA, Christensen DA, Patrick B, Durney CH, Blumenthal DK. The effects of weak extremely low frequency magnetic fields on calcium/calmodulin interactions. Biophys J. 1996; 70:2915-23.

276. Blackman CF, Blanchard JP, Benane SG, House DE. Empirical test of an ion parametric resonance model for magnetic field interactions with PC-12 cells. Bioelectromagnetics. 1994; 15:239-60.

277. Blackman CF, Blanchard JP, Benane SG, House DE. The ion parametric resonance model predicts magnetic field parameters that affect nerve cells. FASEB J. 1995; 9:547-51.

278. Blackman CF, Blanchard JP, Benane SG, House DE, Elder JA. Double blind test of magnetic field effects on neurite outgrowth. Bioelectromagnetics. 1998; 19:204-9.

279. Adair RK. Measurements described in a paper by Blackman, Blanchard, Benane, and House are statistically invalid. Bioelectromagnetics. 1996; 17:510-1.

280. Chiabrera AA, Bianco B, Kaufman JJ, Pilla AA. Quantum analysis of ion binding kinetics in electromagnetic bioeffects. In: "Electromagnetics in Medicine and Biology", CT Brighton, SR Pollack (eds) San Francisco Press Inc. 1991: 27

281. Chiabrera A, Bianco B, Moggia E. Effect of lifetimes on ligand binding modeled by the Density Operator. Bioelectrochemistry Bioenergetics, 1993; 30:35-42.

282. Adair RK. A physical analysis of the ion parametric resonance model. Bioelectromagnetics. 1998; 19:181-91.

283. Liburdy RP, Yost MG. Time-varying and static magnetic fields act in combination to alter calcium signal transduction in the lymphocyte. In: Electricity and Magnetism in Biology and Medicine, (ed. M. Blank) San Francisco Press, 1993, pp. 331-334.

284. Sisken BF, Kanje M, Lundborg G, Kurtz W. Pulsed electromagnetic fields stimulate nerve regeneration in vivo and in vitro. Restorative Neurology. 1990; 1:24-27.

285. Cox JA. Interactive properties of calmodulin. Biochemical Journal. 1988; 249:621-629.

286. Chiabrera A, Bianco B, Kaufman JJ, Pilla AA. Bioelectromagnetic resonance interactions: Endogenous field and noise. In: Interaction Mechanisms of Low-level Electromagnetic Fields. Oxford University Press. 1992, p 164-179.

287. Mehler EL, Pascual-Ahuir J, Weinstein H. Structural dynamics of Calmodulin and Troponin C. Protein Engineering. 1991; 4:625-637.

288. Pilla AA, Muehsam DJ, Markov MS. A dynamical systems/Larmor precession model for weak magnetic field bioeffects: Ion binding and orientation of bound water molecules, Bioelectrochem Bioenergetics. 1997; 43:241-252.

289. Blumenthal DK, Stull JT. Effects of pH, ionic strength, and temperature on activation by calmodulin and catalytic activity of myosin light chain kinase. Biochemistry 1982; 21:2386-91.

290. Pilla AA. Weak static magnetic fields reduce musculoskeletal pain, reduce edema and may enhance human sleep. Bioelectromagnetics Society 25th Annual Meeting, Maui, Hawaii, June 22-26, 2003.

291. Muehsam DJ, Pilla AA. Larmor precession, thermal noise and mechanisms for static magnetic field bioeffects and therapeutic applications. Bioelectromagnetics Society 25th Annual Meeting, Maui, Hawaii, June 22-26, 2003.

292. Foster, K.R. and Schwan, H.P. in C. Polk and E. Postow (eds.), Handbook of Biological Effects of Electromagnetic Fields, CRC Press, Boca Raton, Florida, 1986, p. 83.

293. Adair RK - Constraints on biological effects of weak extremely-low-frequency electromagnetic fields - Phys Rev A 1991; 43: 1038-1049.

294. Weaver JC, Astumian RD. The response of living cells to very weak electric fields: the thermal noise limit. Science. 1990; 247:459-62.

295. Astumian RD, Weaver JC, Adair RK. Rectification and signal averaging of weak electric fields by biological cells. Proc Natl Acad Sci USA. 1995; 92:3740-3.

296. Kruglikov IL, Dertinger H. Stochastic resonance as a possible mechanism of amplification of weak electric signals in living cells. Bioelectromagnetics. 1994;15:539-47.

297. Chiabrera A, Bianco B, Moggia E, Kaufman JJ. Zeeman-Stark modeling of the RF EMF interaction with ligand binding. Bioelectromagnetics 2000; 21:312-324.

298. Doty SB. Morphological evidence of gap junctions between bone cells. Calcif Tissue Int. 1981;33:509.

299. Loewenstein WR. Junctional intracellular communications: the cell-to-cell membrane channel Physiol Rev 1981;61:829-841.

300. McLeod KJ, Lee RC, Ehrlich HP. Frequency dependence of electric field modulation of fibroblast protein synthesis. Science 1987;236:1465-1469.

301. Sheridan JD, Atkinson MM. Cell Membranes: Physiological Roles of Permeable Junctions: Some Possibilities. Ann Rev Physiol. 1985;47:337-353.

302. Adey WR. Cell Membranes: The electrochemical environment and cancer promotion. Neurochem Res. 1988;13:671.

303. Fletcher WH, Shiu WW, Haviland DA, Ware CF, Adey WR. Proc. Bioelectromagnetics Soc., 8th Annual Mtg., Madison, WI, 1986, p.12.

304. Hu GL, Chiang H, Zeng QL, Fu YD. ELF magnetic field inhibits gap junctional intercellular communication and induces hyperphosphorylation of connexin43 in NIH3T3 cells, Bioelectromagnetics, 2001;22:568-573.

305. Lohmann CH, Schwartz Z, Liu Y, Li Z, Simon BJ, Sylvia VL, Dean DD, Bonewald LF, Donahue HJ, Boyan BD. Pulsed electromagnetic fields affect phenotype and connexin 43 protein expression in MLO-Y4 osteocyte-like cells and ROS 17/2.8 osteoblast-like cells. J Orthop Res. 2003;21:326-34.

306. Hopper RA, Mehrara BJ, Lerman OZ, et al. Pulsed electromagnetic fields (PEMF) increase VEGF in cultured osteoblasts. Plastic Surgery Research Council 46th Annual Meeting, Milwaukee, WI; 2001:104.

307. Andrew Lee, W-P. What's new in plastic surgery. J Am Col Surg. 2002;194:324-334.

308. Ramundo-Orlandoa A, Serafinoa A, Schiavoa R, Libertib M, d'Inzeo G. Permeability changes of connexin32 hemi channels reconstituted in liposomes induced by extremely low frequency, low amplitude magnetic fields. BBA-Biomembranes 2005;1668:33-40.

309. Griffin GD, Khalafl W, Hayden KE, Miller EJ, Dowray VR, Creekmore AL, Carruthers CR, Williams MW, Gailey PC. Power frequency magnetic field exposure and gap junctional communication in Clone 9 cells. Bioelectrochemistry 2000;51:117-123.

310. Pilla AA, Nasser PR, Kaufman JJ. The sensitivity of cells and tissues to weak electromagnetic fields. In: "Charge and Field Effects in Biosystems-3", MJ Allen, SF Cleary, AE Sowers, DD Shillady (eds.), Birkhauser, Boston, 1992; 231-41.

311. Pilla AA, Nasser PR, Kaufman JJ. On the sensitivity of cells and tissues to therapeutic and environmental EMF - Bioelectrochemistry and Bioenergetics 1993;30:161-169.

312. Pilla AA, Nasser PR, Kaufman JJ: Gap junction impedance, tissue dielectrics and thermal noise limits for electromagnetic field bioeffects. Bioelectrochem Bioenergetics, 1994;35:63-69.

313. Muehsam DS, Pilla AA. The sensitivity of cells and tissues to exogenous fields: Effects of target system initial state. Bioelectrochem Bioenergetics 1999;48:35-42.

314. Cooper MS. Gap Junctions Increase the Sensitivity of Tissue Cells to Exogenous Electric fields. J Theoret Biol. 1984;111:123-130.

315. Cooper MS. Membrane potential perturbations induced in tissue cells by pulsed electric fields. Bioelectromagnetics. 1995;16:255-62.

316. Hart FX. Cell culture dosimetry for low-frequency magnetic fields. Bioelectromagnetics. 1996; 17:48-57.

317. Fear EC, Stuchly MA. A novel equivalent circuit model for gap-connected cells. Phys Med Biol. 1998; 43:1439-48.

318. Vander Molen MA, Donahue HJ, Rubin CT, McLeod KJ. Osteoblastic networks with deficient coupling: differential effects of magnetic and electric field exposure. Bone. 2000; 27:227-31.

319. Yamaguchi DT, Huang J, Ma D, Wang PK. Inhibition of gap junction intercellular communication by extremely low-frequency electromagnetic fields in osteoblast-like models is dependent on cell differentiation. J Cell Physiol. 2002;190:180-8.

320. Hodgkin AL, Huxley AF, Katz B. Measurement of Current-Voltage Relations in the Membrane of the Giant Axon of Loligo. J Physiol. 1952;116:424-448.

321. Hodgkin AL, Huxley AF. A Quantitative Description of Membrane Current and its Application to Conduction and Excitation in Nerve. J Physiol. 1952;117:500-544.

322. Fishman HM, Poussart DJM, Moore LE, Siebenga E. K^+ Conduction from the Low Frequency Impedance and Admittance of Squid Axon. J Mem Biol. 1977;32:255-290.

323. Fishman HM, Poussart DJM, Moore LE. Complex Admittance of Na^+ Conduction in Squid Axon. J Mem Biol. 1979;50:43-63.

324. Fishman HM, Leuchtag HR, Moore LE. Fluctuation and Linear Analysis of Na-Current Kinetics in Squid Axon. Biophys J. 1983;43:293-307.

325. Angerbauer, G.J., 1989. Principles of DC and AC Circuits, 3rd Edition, Delmar Publishers, Albany, NY p. 490.

326. Stevens CF. Inferences about membrane properties from electric noise measurements. Biophys J. 1972;12:1028-47.

327. DeFelice LJ. Introduction to Membrane Noise, Plenum, NY, 1981, pp. 243-45.

328. Daff S. Calmodulin-dependent regulation of mammalian nitric oxide synthase. Biochem Soc Trans. 2003;31:502-5.

329. Damy T, Ratajczak P, Shah AM, Camors E, Marty I, Hasenfuss G, Marotte F, Samuel JL, Heymes C. Increased neuronal nitric oxide synthase-derived NO production in the failing human heart. Lancet. 2004; 363:1365-7.

330. Angerbauer GJ. Principles of DC and AC Circuits, 3rd Edition, Delmar Publishers, Albany, NY 1989, p. 490.

331. Paul RG, Tarlton JF, Purslow PP, Sims TJ, Watkins P, Marshall F, M. J. Ferguson MJ, Bailey AJ. Biomechanical and Biochemical Study of a Standardized Wound Healing Model. Int J Biochem Cell Biol. 1997; 29:211-220.

332. Glassman LS, McGrath MH, Bassett CA. Effect of external pulsing electromagnetic fields on the healing of soft tissue. Ann Plastic Surg. 1986; 16:287-195.

333. Patel M, Yu H, Strauch B. Effects of pulsed magnetic field treatment on the healing of linear incision wounds. Plastic Surgery Research Council, Toronto, Canada, May, 2005.

334. Yamauchi T, Yoshimura Y, Nomura T, Fujii M, Sugiura H. Neurite outgrowth of neuroblastoma cells overexpressing alpha and beta isoforms of Ca2+/calmodulin-dependent protein kinase II: effects of protein kinase inhibitors. Brain Res Brain Res Protoc. 1998;2:250-258.

335. Sisken BF, Kanje M, Lundborg G, Kurtz W. Pulsed electromagnetic fields stimulate nerve regeneration in vivo and in vitro. Restorative Neurology Neuroscience, 1990;1:303-309.

336. Greenbaum B, Sutton C, Vadula MS, Battocletti JH, Swiontek T, DeKeyser J, Sisken B. Effects of pulsed magnetic fields on neurite outgrowth from chick embryos. Bioelectromagnetics, 1996;17:293-302.

337. Sisken BF, Kanje M, Lundborg G, Kurtz W. Pulsed electromagnetic fields stimulate nerve regeneration in vivo and in vitro. Restorative Neurology and Neuroscience, 1990;1:303-309.

338. Diniz P, Shomura K, Soejima K, Ito G. Effects of pulsed electromagnetic field (PEMF) stimulation on bone tissue like formation are dependent on the maturation stages of the osteoblasts. Bioelectromagnetics 2002;23:398-405.

339. Muehsam DS, Pilla AA. The Sensitivity of Cells and Tissues to Exogenous Fields: Effects of Target System Initial State. Bioelectrochem Bioenergetics, 1999;48:35-42.

340. Nindl G, Swezb JA, Millera JM, Balcavage WX. Growth stage dependent effects of electromagnetic fields on DNA synthesis of Jurkat cells. FEBS Letters 1997;414:501-506.

341. Longo JA. The management of recalcitrant nonunions with combined magnetic field stimulation. Orthop Trans. 1998; 22:408-409.

342. Norton L, Pilla A, Regelson W, Tansman L. J Electrochem Soc. 1980; 127:130C.

343. Norton L, Tansman L, Regelson W. J Electrochem Soc. 1982; 129:132C.

344. Tofani S, Cintorino M, Barone D, Berardelli M, De Santi MM, Ferrara A, Orlassino R, Ossola P, Rolfo K, Ronchetto F, Tripodi SA, Tosi P. Increased mouse survival, tumor growth inhibition and decreased immunoreactive p53 after exposure to magnetic fields. Bioelectromagnetics. 2002; 23:230-8.

345. Tofani S, Barone D, Berardelli M, Berno E, Cintorino M, Foglia L, Ossola P, Ronchetto F, Toso E, Eandi M. Static and ELF magnetic fields enhance the in vivo anti-tumor efficacy of cis-platin against lewis lung carcinoma, but not of cyclophosphamide against B16 melanotic melanoma. Pharmacol Res. 2003; 48:83-90.

346. Salvatore JR, Harrington J, Kummet T. Phase I clinical study of a static magnetic field combined with anti-neoplastic chemotherapy in the treatment of human malignancy: initial safety and toxicity data. Bioelectromagnetics. 2003; 24:524-7.

347. Plotnikov A, Fishman D, Tichler T, Korenstein R, Keisari Y. Low electric field enhanced chemotherapy can cure mice with CT-26 colon carcinoma and induce anti-tumour immunity. Clin Exp Immunol. 2004; 138:410-6.

348. Johnson MT, Waite LR, Nindl G. Noninvasive treatment of inflammation using electromagnetic fields: current and emerging therapeutic potential. Biomed Sci Instrum. 2004; 40:469-74.

349. Ronchetto F, Barone D, Cintorino M, Berardelli M, Lissolo S, Orlassino R, Ossola P, Tofani S. Extremely low frequency-modulated static magnetic fields to treat cancer: A pilot study on patients with advanced neoplasm to assess safety and acute toxicity. Bioelectromagnetics. 2004; 25:563-71.

350. Trillo A, Ubeda A, Blanchard JP, House DE, Blackman CF. Magnetic fields at resonant conditions for the hydrogen ion affect neurite outgrowth in PC-12 cells. Bioelectromagnetics 1996;17:10–20.

351. Baureus Koch CL, Sommarin M, Persson BR, Salford LG, Eberhardt JL. Interaction between weak low frequency magnetic fields and cell membranes. Bioelectromagnetics. 2003;24:395-402.

352. Tuffet S, de Seze R, Moreau JM, Veyret B. Effects of a strong pulsed magnetic field on the proliferation of tumor cells in vitro. Bioelectrochem Bioenerg. 1993;30:151-160.

353. Fanelli C, Coppola S, Barone R, Colussi C, Gualardi G, Volpe P, Ghibelli L. Magnetic fields increase cell survival by inhibiting apoptosis via modulation of Ca^{2+} influx. FASEB J. 1999;13:95-102.

354. Belyaev IY, Matronchik AY, Alipov YD. 1994. The effect of weak static and alternating magnetic fields on the genome conformational state of E. coli cells: The evidence for model of phase modulation of high frequency oscillations. In: Allen MJ, editor. Charge and Field effects in biosystems-4. World Scientific, Singapore. p 174-184.

355. Binhi VN, Alipov YD, Belyaev IY. Effect of static magnetic field on E. coli cells and individual rotations of ion-protein complexes. Bioelectromagnetics. 2001;22:79-86.

356. Cameron IL, Sun LZ, Short N, Hardman WE, Williams CD. Therapeutic Electromagnetic Field (TEMF) and Gamma Irradiation on Human Breast Cancer Xenograft Growth, Angiogenesis and Metastasis. Cancer Cell Int. 2005;5:23.

357. Fini M, Giavaresi G, Torricelli P, Cavani F, Setti S, Cane V, Giardino R. Pulsed electromagnetic fields reduce knee osteoarthritic lesion progression in the aged Dunkin Hartley guinea pig. J Orthop Res. 2005;23:899-908.

358. McCaig CD, Rajnicek AM, Song B, Zhao M. Controlling cell behavior electrically: current views and future potential. Physiol Rev. 2005;85:943-78.

359. Thamsborg G, Florescu A, Oturai P, Fallentin E, Tritsaris K, Dissing S. Treatment of knee osteoarthritis with pulsed electromagnetic fields: a randomized, double-blind, placebo-controlled study. Osteoarthritis Cartilage. 2005;13:575-81.

360. Morris C, Skalak T. Static magnetic fields alter arteriolar tone in vivo. Bioelectromagnetics. 2005;26:1-9.

361. De Pedro JA, Perez-Caballer AJ, Dominguez J, Collia F, Blanco J, Salvado M. Pulsed electromagnetic fields induce peripheral nerve regeneration and endplate enzymatic changes. Bioelectromagnetics. 2005;26:20-7.

362. Zborowski M, Midura RJ, Wolfman A, Patterson T, Ibiwoye M, Sakai Y, Grabiner M. Magnetic field visualization in applications to pulsed electromagnetic field stimulation of tissues. Ann Biomed Eng. 2003;31:195-206.

363. Ibiwoyea MO, Powella KA, Grabinera MD, Patterson TE, Sakaia Y, Zborowskia M, Wolfmanc A, Midura RJ. Bone mass is preserved in a critical-sized osteotomy by low energy pulsed electromagnetic fields as quantitated by in vivo micro-computed tomography. J Orthop Res. 2004;22:1086–1093.

364. King RW. Nerves in a human body exposed to low-frequency electromagnetic fields. IEEE Trans Biomed Eng. 1999;46:1426-31.

365. Cooper MS, Miller JP, Fraser SE. Electrophoretic repatterning of charged cytoplasmic molecules within tissues coupled by gap junctions by externally applied electric fields. Dev Biol. 1989;132:179-88.

366. Gowrishankar TR, Weaver JC. An approach to electrical modeling of single and multiple cells. Proc Natl Acad Sci U S A. 2003;100:3203-8.

367. Fear EC, Stuchly MA. Modeling assemblies of biological cells exposed to electric fields. IEEE Trans Biomed Eng. 1998;45:1259-71.

368. Fear EC, Stuchly MA. Biological cells with gap junctions in low-frequency electric fields. IEEE Trans Biomed Eng. 1998;45:856-66.

369. Midura RJ, Ibiwoye MO, Powell KA, Sakai Y, Doehring T, Grabiner MD, Patterson TE, Zborowski M, Wolfman A. Pulsed electromagnetic field treatments enhance the healing of fibular osteotomies. J Orthop Res. 2005 Jun 2; [Epub ahead of print]

370. Segal NA, Toda Y, Huston J, Saeki Y, Shimizu M, Fuchs H, Shimaoka Y, Holcomb R, McLean MJ. Two configurations of static magnetic fields for treating rheumatoid arthritis of the knee: a double-blind clinical trial. Arch Phys Med Rehabil. 2001;82:1453-60.

371. Hinman MR, Ford J, Heyl H. Effects of static magnets on chronic knee pain and physical function: a double-blind study. Altern Ther Health Med. 2002;8:50-5.

372. Weaver J. This volume.

373. Cho CK. This volume.

374. Liboff A. This volume.

375. Wolff J. [The law of bone remodeling]. Berlin: Hirshwald; 1892. p 17-35. German.

376. Huiskes R, Ruimerman R, van Lenthe GH, Janssen JD. Effects of mechanical forces on maintenance and adaptation of form in trabecular bone. Nature. 2000;405:704-6.

377. Fritton SP, McLeod KJ, Rubin CT. Quantifying the strain history of bone: spatial uniformity and self-similarity of low-magnitude strains. J Biomech, 2000;33:317-25.

378. Huang RP, Rubin CT, McLeod KJ. Changes in postural muscle dynamics as a function of age. J Gerontol A Biol Sci Med Sci. 1999;54:B352-7.

379. Goodship AE, Lawes T, Rubin CT. Low magnitude high frequency mechanical stimulation of endochondral bone repair. Trans Orthop Res Soc. 1997;22:234.

380. Goodship AE, Kenwright J. The influence of induced micromovement upon the healing of experimental tibial fractures. J Bone Joint Surg Br. 1985;67:650-5.

381. Busse JW, Bhandari M, Kulkarni AV, Tunks E. The effect of low-intensity pulsed ultrasound therapy on time to fracture healing: a meta-analysis. CMAJ. 2002; 166:437-41.

382. Azuma Y, Ito M, Harada Y, Takagi H, Ohta T, Jingushi S. Low-intensity pulsed ultrasound accelerates rat femoral fracture healing by acting on the various cellular reactions in the fracture callus. J Bone Miner Res. 2001;16:671-80.

383. Parvizi J, Wu CC, Lewallen DG, Greenleaf JF, Bolander ME. Low-intensity ultrasound stimulates proteoglycan synthesis in rat chondrocytes by increasing aggrecan gene expression. J Orthop Res. 1999;17:488-94.

384. Korstjens CM, Nolte PA, Burger EH, Albers GH, Semeins CM, Aartman IH, Goei SW, Klein-Nulend J. Stimulation of bone cell differentiation by low-intensity ultrasound--a histomorphometric in vitro study. J Orthop Res. 2004;22:495-500.

385. Wang N, Butler JP, Ingber DE. Mechanotransduction across the cell surface and through the cytoskeleton. Science 1993;260:1124–7.

386. Kokubu T, Matsui N, Fujioka H, Tsunoda M, Mizuno K. Low intensity pulsed ultrasound exposure increases prostaglandin E2 production via the induction of cyclooxygenase-2 mRNA in mouse osteoblasts. Biochem. Biophys. Res. Commun. 1999;256:284–287.

387. Naruse K, Mikuni-Takagaki Y, Azuma Y, Ito M, Ohta T, Kameyama K-Z, Itoman M. Anabolic response of mouse bone-marrow-derived stromal cell clonal ST2 cells to low intensity pulsed ultrasound. Biochem Biophys Res Commun. 2000;268:216–220.

388. Warden SJ, Favaloro JM, Bennell KL, McMeeken JM, Ng KW, Zajac JD, Wark JD. Low-intensity pulsed ultrasound stimulates a bone-forming response in UMR-106 cells. Biochem Biophys Res Commun. 2001;286:443-50.

389. Parvizi J, Parpura V, Greenleaf JF, Bolander ME. Calcium signaling is required for ultrasound-stimulated aggrecan synthesis by rat chondrocytes. J Orthop Res. 2002;20:51-7.

390. Wang FS, Kuo YR, Wang CJ, Yang KD, Chang PR, Huang YT, Huang HC, Sun YC, Yang YJ, Chen YJ. Nitric oxide mediates ultrasound-induced hypoxia-inducible factor-1alpha activation and vascular endothelial growth factor-A expression in human osteoblasts. Bone. 2004;35:114-23.

391. De Mattei M, Pasello M, Pellati A, Stabellini G, Massari L, Gemmati D, Caruso A. Effects of electromagnetic fields on proteoglycan metabolism of bovine articular cartilage explants. Connect Tissue Res. 2003;44:154-9.

392. Li H, Poulos TL. Structure-function studies on nitric oxide synthases. J Inorg Biochem. 2005;99:293-305.

393. Pitsillides AA, Rawlinson SC, Suswillo RF, Bourrin S, Zaman G, Lanyon LE. Mechanical strain-induced NO production by bone cells: a possible role in adaptive bone (re)modeling? FASEB J. 1995;9:1614-22.

394. Ignarro LJ, Napoli C. Novel features of nitric oxide, endothelial nitric oxide synthase, and atherosclerosis. Curr Diab Rep. 2005;5:17-23.

395. Bockris JO,. Saluja PPS. Ionic Solvation Numbers from Compressibilities and Ionic Vibration Potentials Measurements J Phys Chem. 1972;76;2140-2151.

396. Buchanan TJ, Haggis GH, Hasted JB, Robinson BG. The Dielectric Estimation of Protein Hydration, Proc Roy Soc London 1952;A213:379-391.

397. Conway BE. Ionic Hydration in Chemistry and Biophysics, Elsevier, New York, 1981.

398. Termaat MF, Den Boer FC, Bakker FC, Patka P, Haarman HJ. Bone morphogenetic proteins. Development and clinical efficacy in the treatment of fractures and bone defects. J Bone Joint Surg Am. 2005;87:1367-78.

399. Bennett SP, Griffiths GD, Schor AM, Leese GP, Schor SL. Growth factors in the treatment of diabetic foot ulcers. Br J Surg. 2003;90:133-46.